HRTEM and STEM Image Simulation

Winter School on High Resolution Electron Microscopy
at Arizona State University
January 4 - 8, 2016

Pierre Stadelmann
JEMS-SAAS
CH-3906 Saas-Fee
Switzerland

December 14, 2015

How to do diffraction/image simulation?

Formation of Electron Microscopy diffraction/images involves complex physical processes.

Approximations and models of these physical processes

are required in order to perform computer simulations. Models are based on electron scattering, diffraction, optics, ...

Needed: crystallography, optics, quantum mechanics, ... and computer programming.

TEM (very) simplified model

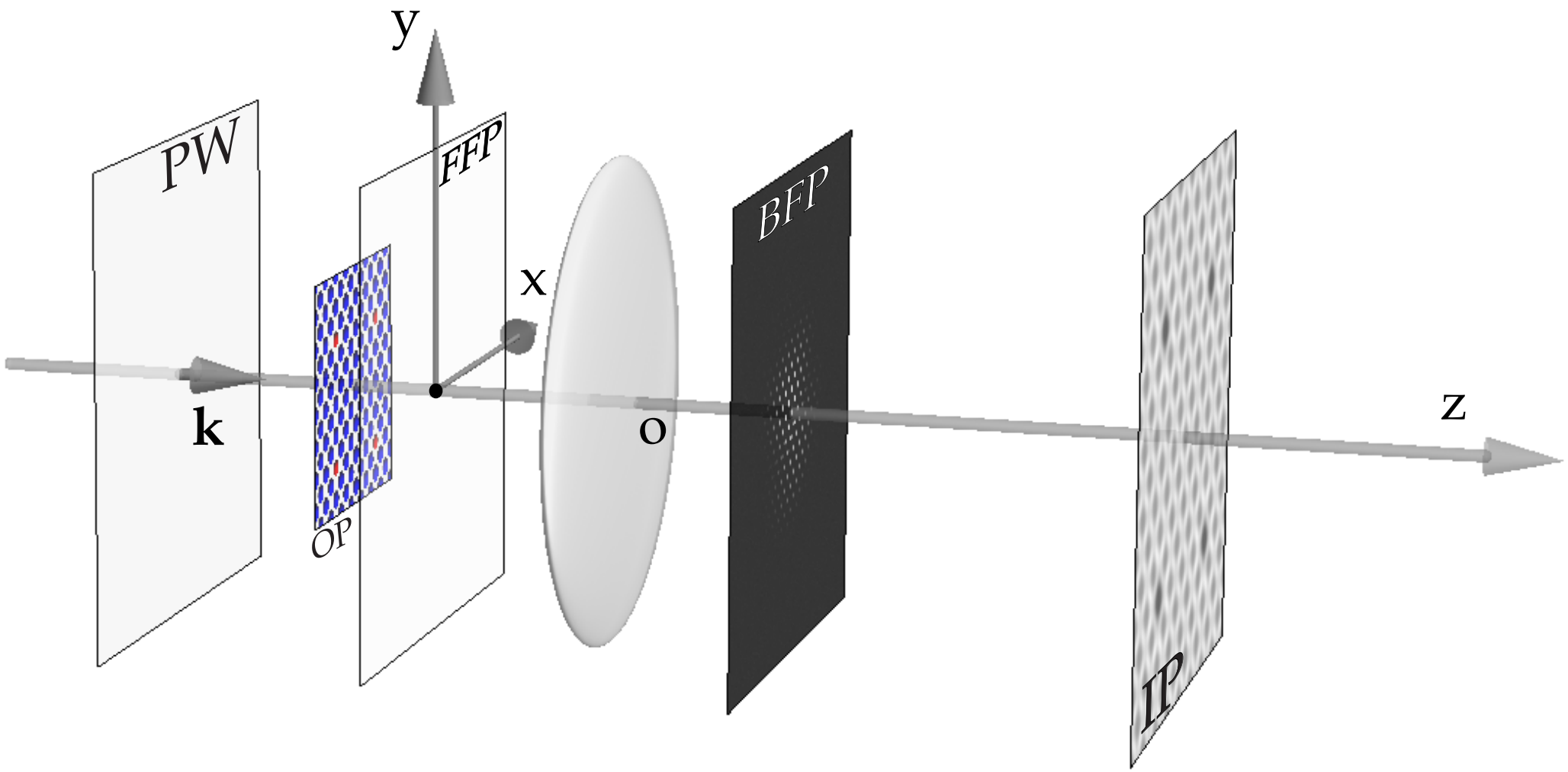

Modeling steps: Incident wave (PW), crystal (OP), electron-matter interaction, Fraunhofer approximation, image formation (Abbe theory), ...

Image formation modeling (HRTEM)

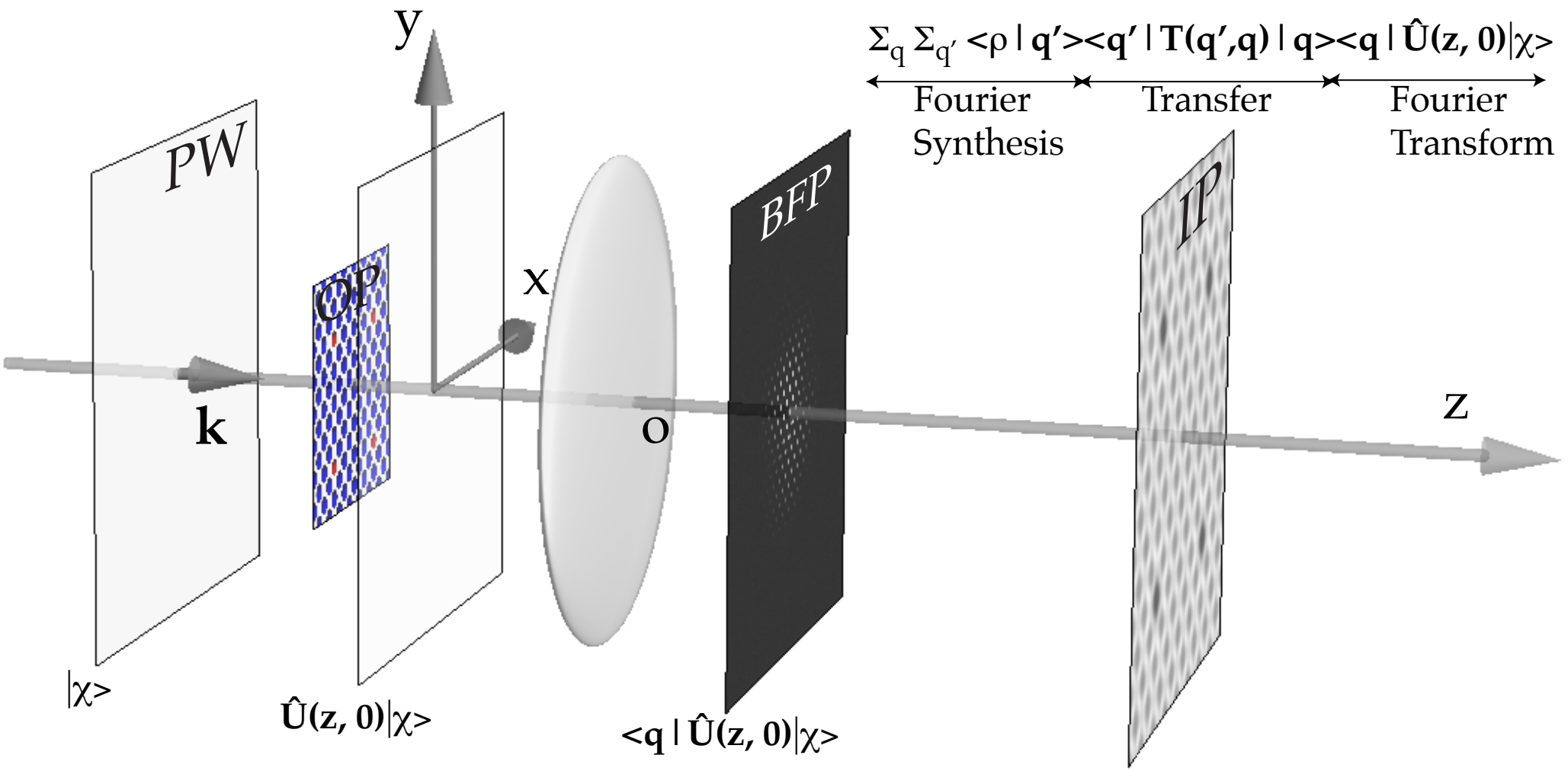

Image wave function: $|\Psi_i>$

$$|\chi> \implies \text{incident wave function}$$

$$|\Psi_i> = \underbrace{\sum^{q'} <\rho|q'>}_{\text{Fourier synthesis}} \underbrace{\sum^{q} <q'|T(q',q)|q>}_{\text{Objective lens transfer}} \underbrace{<q|U(z,0)|\chi>}_{\text{Fourier transform}}$$

Assuming that the potential is z independent, the evolution operator $U(z,0)$ depends on the Hamiltonian $H(\vec{\rho},z)$ of the system "crystal + incident electron" (where $\vec{\rho}$ are the (x, y) coordinates in a plane perpendicular to the optical axis O_z of the microscope):

$$U(z,0) = \exp^{-i\int_0^z H(\vec{\rho},z)dz}$$

The main problem of high-energy electron diffraction and imaging is to determine $U(z,0)$.

Modeling steps

Prior to perform any calculation the following items (from the electron source to the detector) must characterized and modeled:

- The electron beam properties.
  - Convergence.
  - Source size.
  - Coherence (spatial and temporal).
- The specimen properties.
- How is the incident electrons beam scattered by the specimen?
- How does the microscope transfer the scattered electron beam?
- How do we measure the properties of the scattered electron beam (diffraction, image, hologram)?
- What are the properties of the detection system?

Modelling steps

- Object:
  - crystal structure.
  - crystal orientation.
  - crystal shape.
- Scattering & Diffraction:
  - incident wave-function.
  - evolution operator.
  - exit wave-function.
- Image Formation:
  - HRTEM: Transfer Function (TF) or Transmission Cross Coefficients (TCC).
  - HRSTEM: Optical Transfer Function (OTF).
- Image acquisition:
  - characterisation of the Modulation Transfer Function (MTF) of the detector.

Modelling the object

Evolution operator U (z, 0) depends on the object properties

1. Amorphous material or crystalline material.
2. Thin or thick.
3. Orientation (high or low symmetry [uvw]).

You might have to transform the unit cell in order to perform dynamical calculations[1].

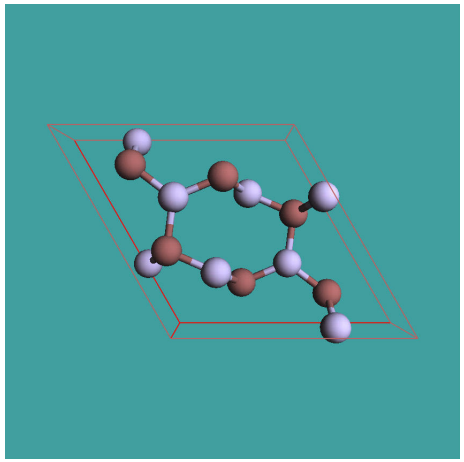

Si_3N_4 hexagonal lattice.

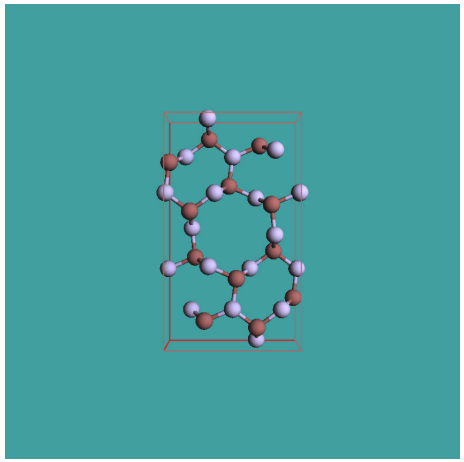

Si_3N_4 orthorhombic lattice.

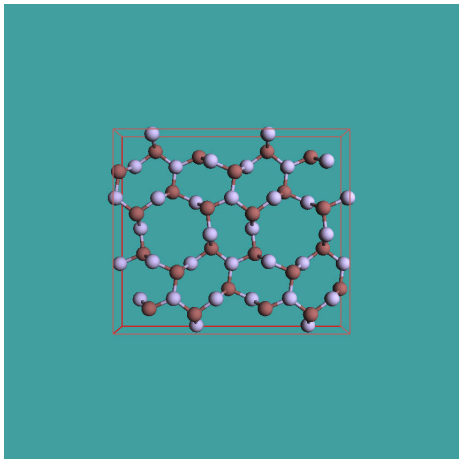

Si_3N_4 orthorhombic lattice x 2.

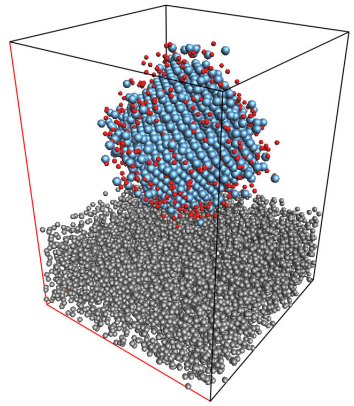

Pt catalyst on amorphous carbone film (9600 atoms).

Any model is considered a periodic unit cell independent of its complexity.

[1] See International Tables for Crystallography (1992) Vol. 1, Chapter 5.

Atomic scattering amplitude

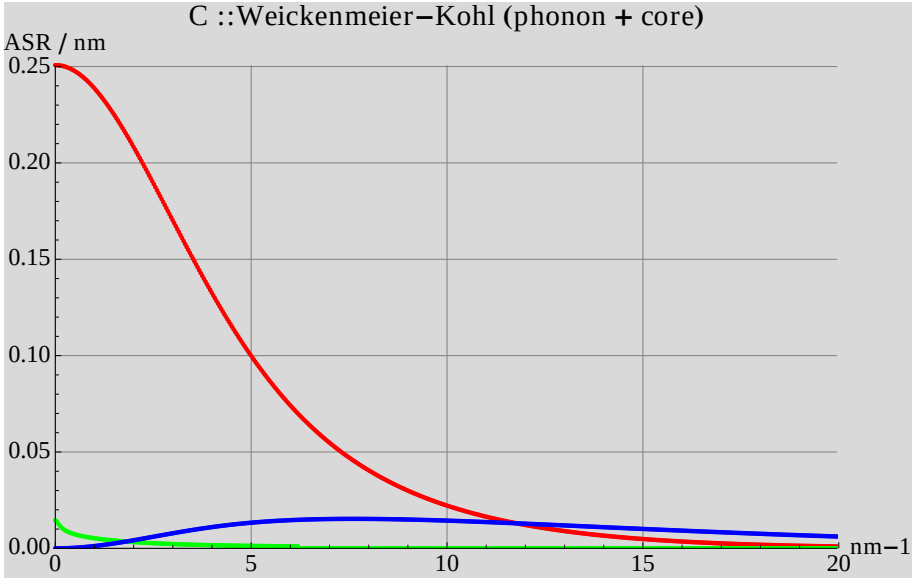

Carbon. red: real part, green: imaginary part, blue: thermal diffuse scattering.

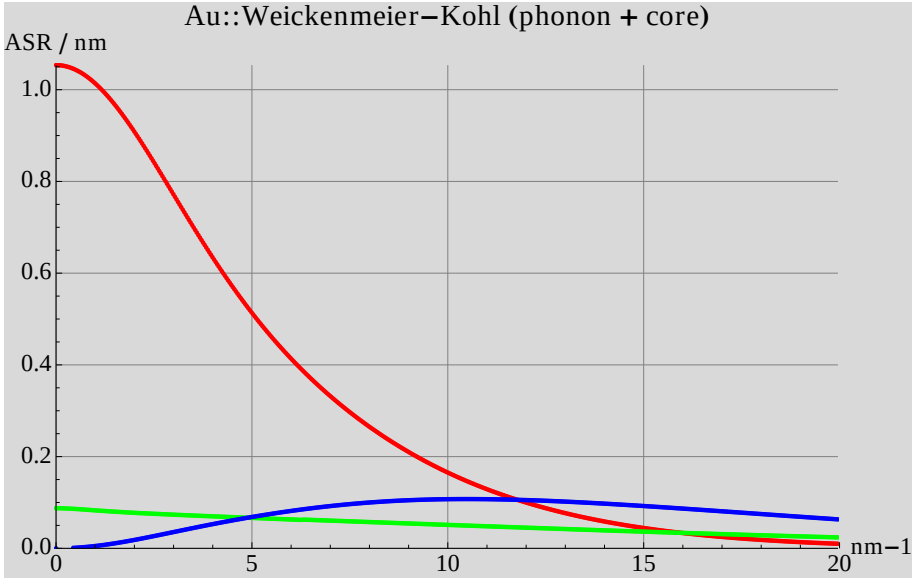

Gold. red: real part, green: imaginary part, blue: thermal diffuse scattering.

The TDS (Thermal Diffuse Scattering) at large s ($=\sin(\theta)$) scales as $\approx Z^{1.7}$. It explains HAADF (High Angle Annular Dark Field) atomic column contrast.

Atomic form factors

Atomic form factors have been tabulated by many authors:

1. Doyle-Turner and Smith-Burge.
2. E.J. Kirkland.
3. Peng-Ren-Dudarev-Whelan.
4. ...

Take care ASA of heavy atoms aren't always tabulated properly.

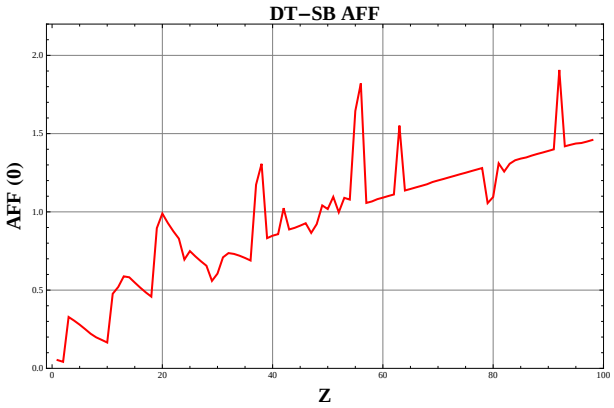

Doyle-Turner or Smith-Burger.

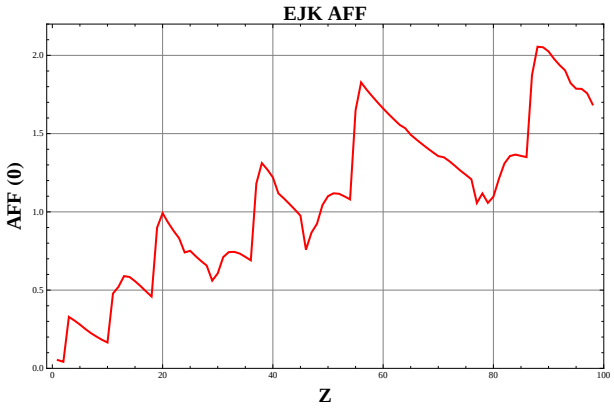

E. J. Kirkland.

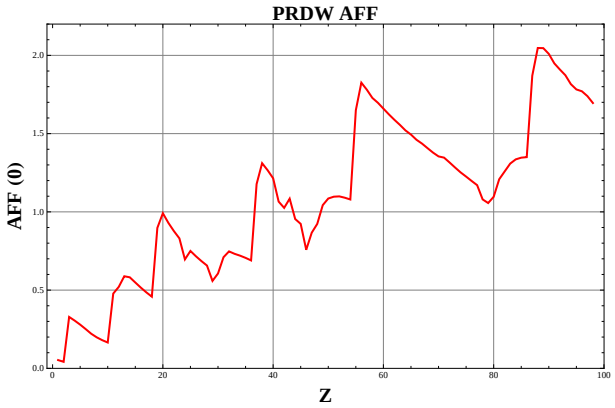

Peng-Ren-Dudarev-Whelan.

A extremely useful ASA tabulation including phonon and core loss absorption is due to Weickenmeier-Kohl[2].

[2] A. Weickenmeier, H. Kohl, Acta Cryst. A 47 (1991) 590.

Atomic form factors

Crystal structure are defined by:

1. a, b, c, α, β, γ lattice parameters.
2. Space-group or symmetry operators.
3. Atoms positions (Symbol, x, y, z with $0 \leq$ (x, y, z) < 1)

$> 10^5$ crystal structures provided by data bases (ICSD, Min. Soc. Ame., Cryst. Open Database).

Useful severs:
www.minsocam.org
www.crystallography.net
www.cryst.ehu.es

ICSD & AMS: data bases for crystal structures

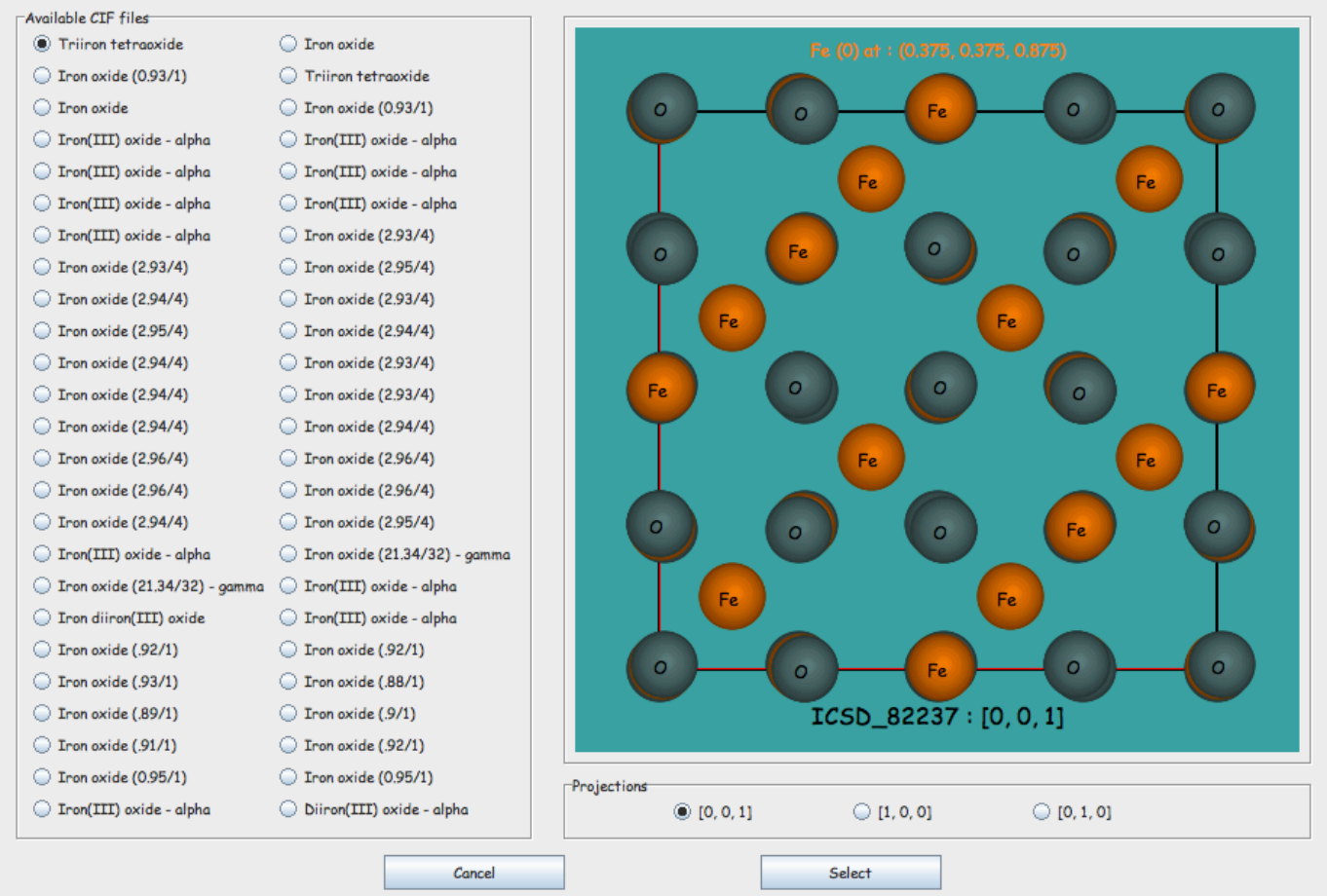

Scattering & diffraction

Scattering: electron-matter interaction

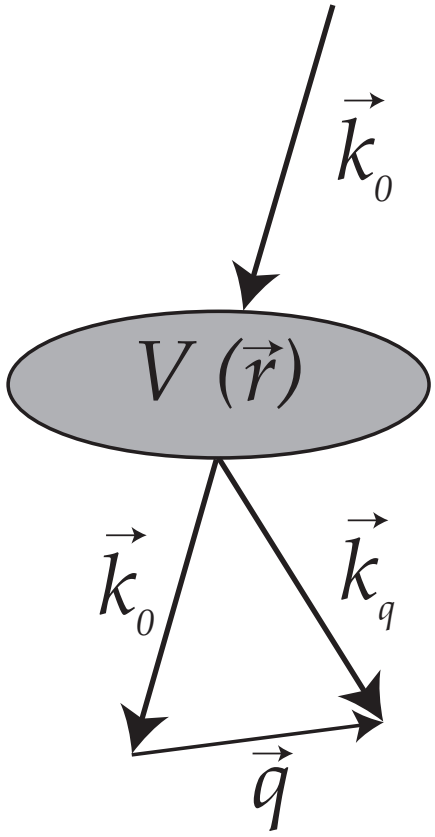

An incident electron of wave vector $\vec{k}_0$ interacts with a solid of scalar potential $V(\vec{r})$. The wave vector of the scattered electron is $\vec{k}_q = \vec{k}_0 + \vec{q}$ where $\vec{q}$ is the momentum transfered by the solid[3].

$$\text{Elastic scattering} \longrightarrow ||\vec{k}_q|| = ||\vec{k}_0||.$$

[3] Magnetic and spin effects are ignored.

Diffraction: Bragg law

With energy conservation and momentum transfer ($\vec{s_g} = 0$), i.e. elastic scattering:

$$|\vec{k_i} + \vec{g}| = |\vec{k_g}|$$

$$k_i^2 + 2 \times k_i \times g \times \cos(\vec{k_i}, \vec{g}) + g^2 = k_g^2$$

$$2k_i \times \cos(\vec{k_i}, \vec{g}) = -g$$

$$2k_i \times \cos(90^o - \theta_B) = -g$$

$$\frac{2}{\lambda} \times \sin(\theta_B) = g = \frac{1}{d_g}$$

$\Longrightarrow$ Bragg law:

$$2 \times d_{hkl} \times \sin(\theta_B) = \lambda$$

Diffraction geometry: small angle approximation

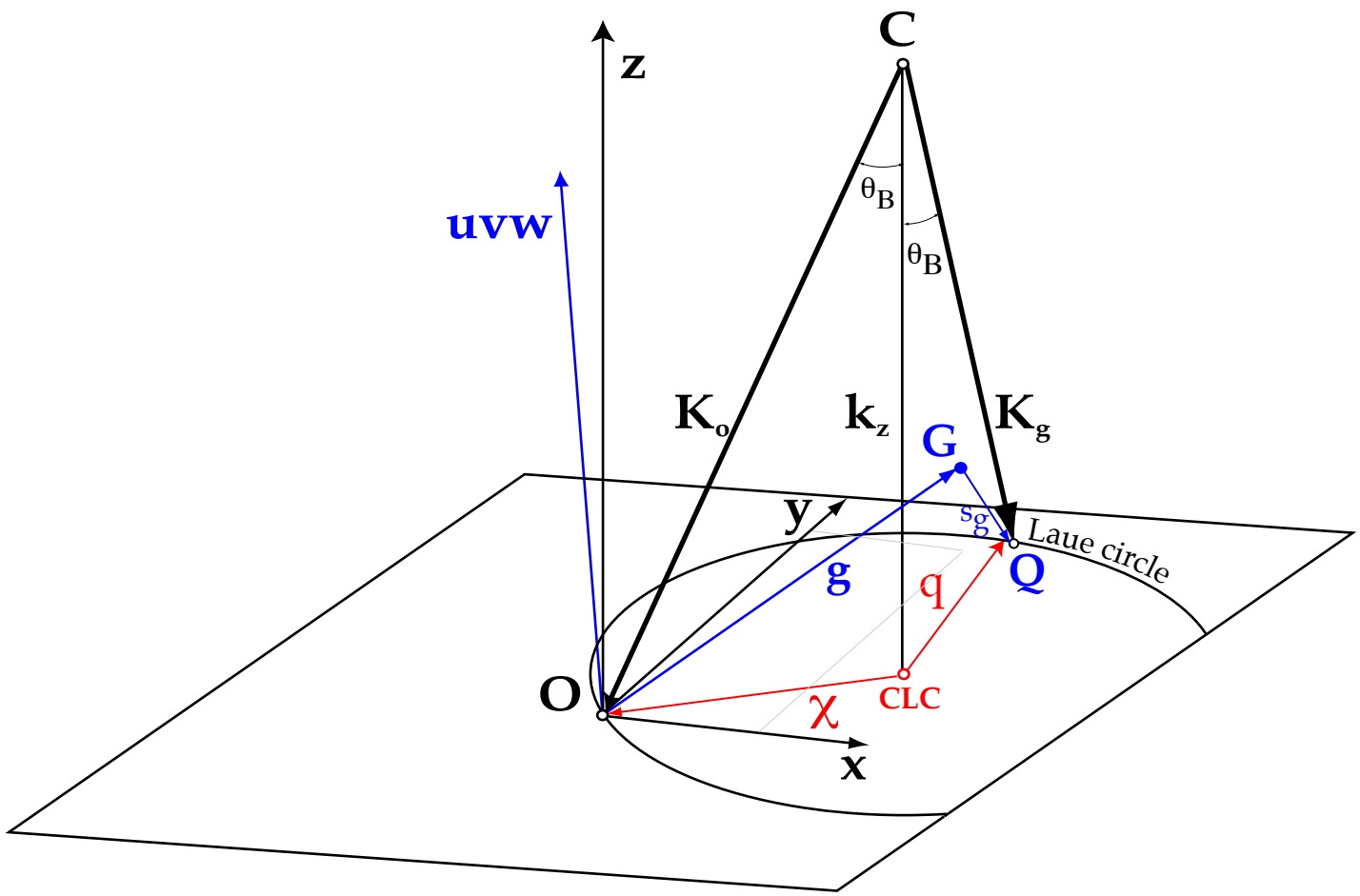

Center of the Ewald sphere (C) and Center of the Laue Circle (CLC), projection of C onto the zero order Laue zone. All reflections on the circle of radius χ are at exact Bragg condition. Notice that the Bragg angles are pretty small (of the order a few ^{o}) and that consequently the small angle approximation is quite good.

Structure factors

The structure factor gives the scattering *strength* of (h,k,l) planes.

$$F_{hkl} = \sum_{i=atomes} f_i(s_{hkl}) e^{(2\pi\imath(hx_i+ky_i+lz_i))}$$

where:

1. $f_i(s_{hkl})$ is the atomic scattering amplitude.
2. (x_i, y_i, z_i) are the fractional coordinates of atom i $(0 \leq x_i < 1)$.
3. $s_{hkl} = \frac{sin(\theta_B)}{\lambda} = \frac{1}{2d_{hkl}}$.

In general all reflections allowed by the Bravais lattice are visible:
Simple cubic: (hkl) no condition.
1 atom at (0, 0, 0).

$$\Longrightarrow F_{hkl} = f_i(s_{hkl})$$

Body centered cubic: $(hkl) : h + k + l = 2n$
2 atoms at (0,0,0) and $(\frac{1}{2}, \frac{1}{2}, \frac{1}{2})$.

$$\Longrightarrow F_{hkl} = f_i(s_{hkl}) \left[1 + e^{\pi\imath(h+k+l)}\right]$$

Face centered cubic: (hkl) all even or odd.
4 atoms at $(0, 0, 0)$, $(0, \frac{1}{2}, \frac{1}{2})$, $(\frac{1}{2}, 0, \frac{1}{2})$, $(\frac{1}{2}, \frac{1}{2}, 0)$

$$\Longrightarrow F_{hkl} = f_i(s_{hkl}) \left[1 + e^{\pi\imath(h+k)} + e^{\pi\imath(h+l)} + e^{\pi\imath(k+l)}\right]$$

Kinematical diffraction: $< q|U(z,0)|\chi >$

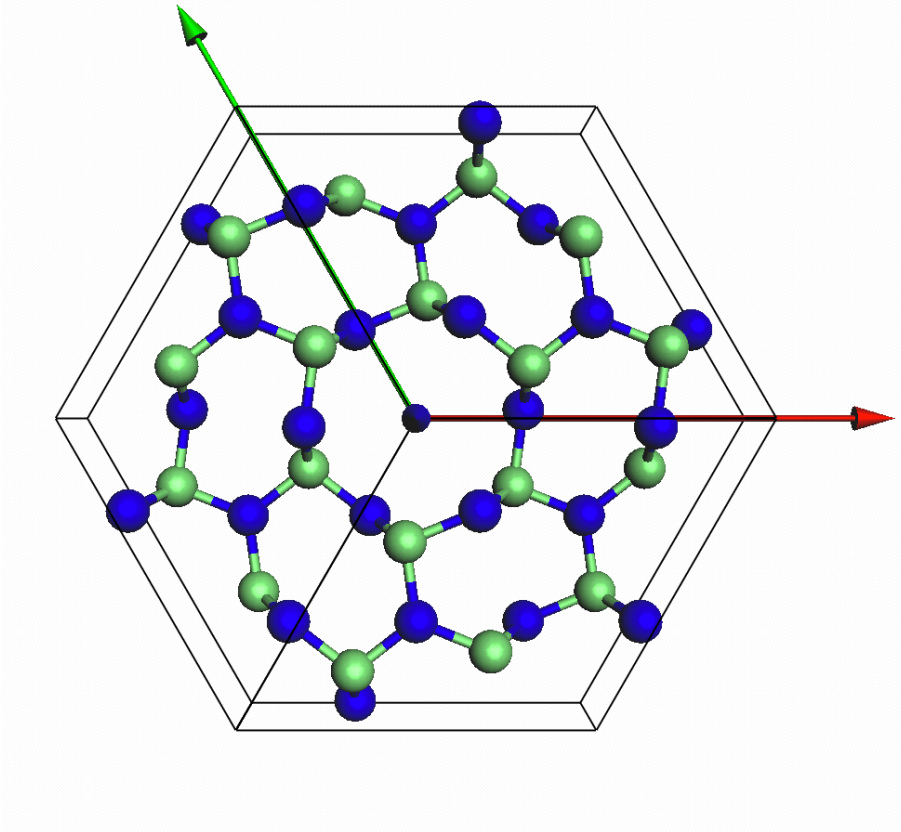

Figure : Model (Ge_3N_4).

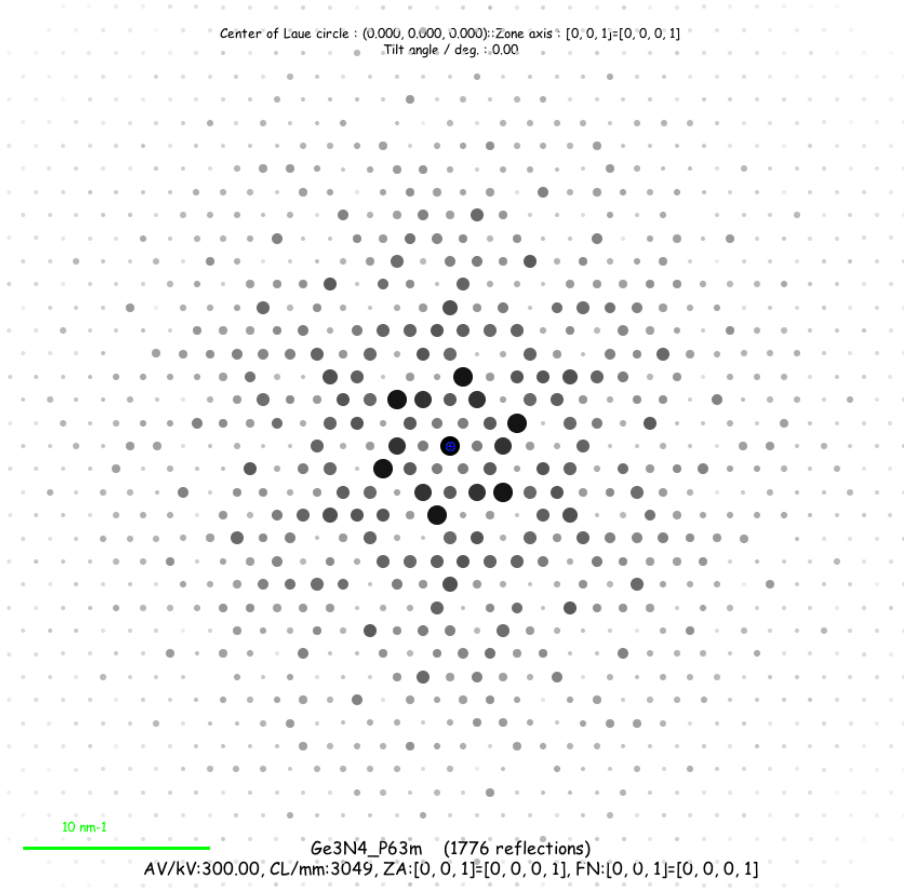

Figure : Kinematical diffraction Ge_3N_4, [001].

Dynamical diffraction: $< q|U(z,0)|\chi >$

$< q|U(z,0)|\chi > \implies$ Fourier transform of object wavefunction

Dynamical scattering (many approaches under small angle approximation and elastic scattering).
Including inelastic scattering more complicated and computer intensive.

Gratias & Portier: small angle & elastic scattering approximations

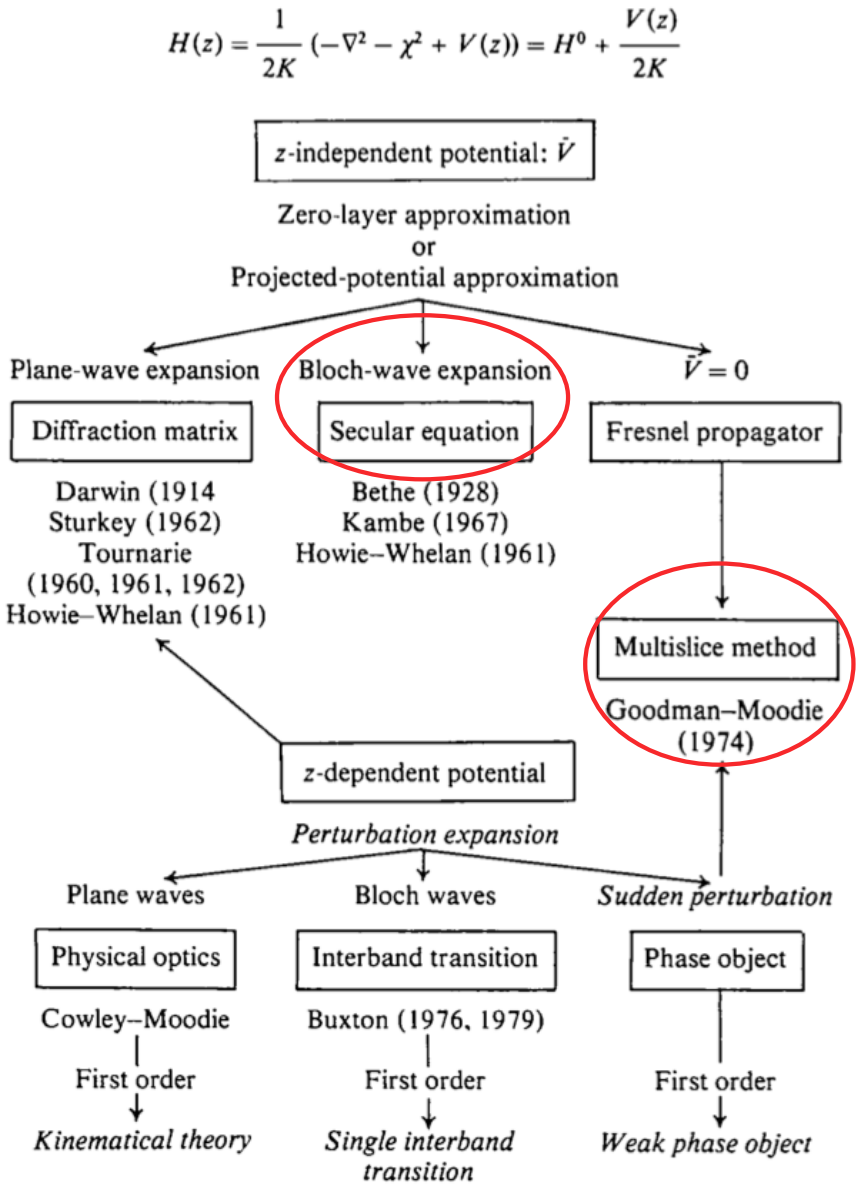

From Gratias and Portier[4].

[4] D. Gratias and R. Portier, Time-Like Perturbation Method in High-Energy Electron Diffraction, Acta Cryst. **A39** (1983) 576-584

The two most employed calculation methods

All approximations are numerically equivalent, but perform best in particular cases.
We will consider only 2 approximations:

- The multislice approximation[5].
- The Bloch-wave method[6].

The multislice method performs best when simulating crystalline or amorphous solids of large unit cell or containing defects while the Bloch-wave method is adapted to the calculation of crystalline solids of small unit cell and in any [uvw] orientation. The Bloch-wave method has also several advantages (speed, ease of use) for simulating CBED, LACBED or PED patterns and for polarity and chirality determination.

[5] J. Cowley and A.F. Moodie, Proc. Phys. Soc. B70 (1957) 486, 497 and 505.

[6] H. A. Bethe, Ann. Phys. 87 (1928), 55.

Multislice method

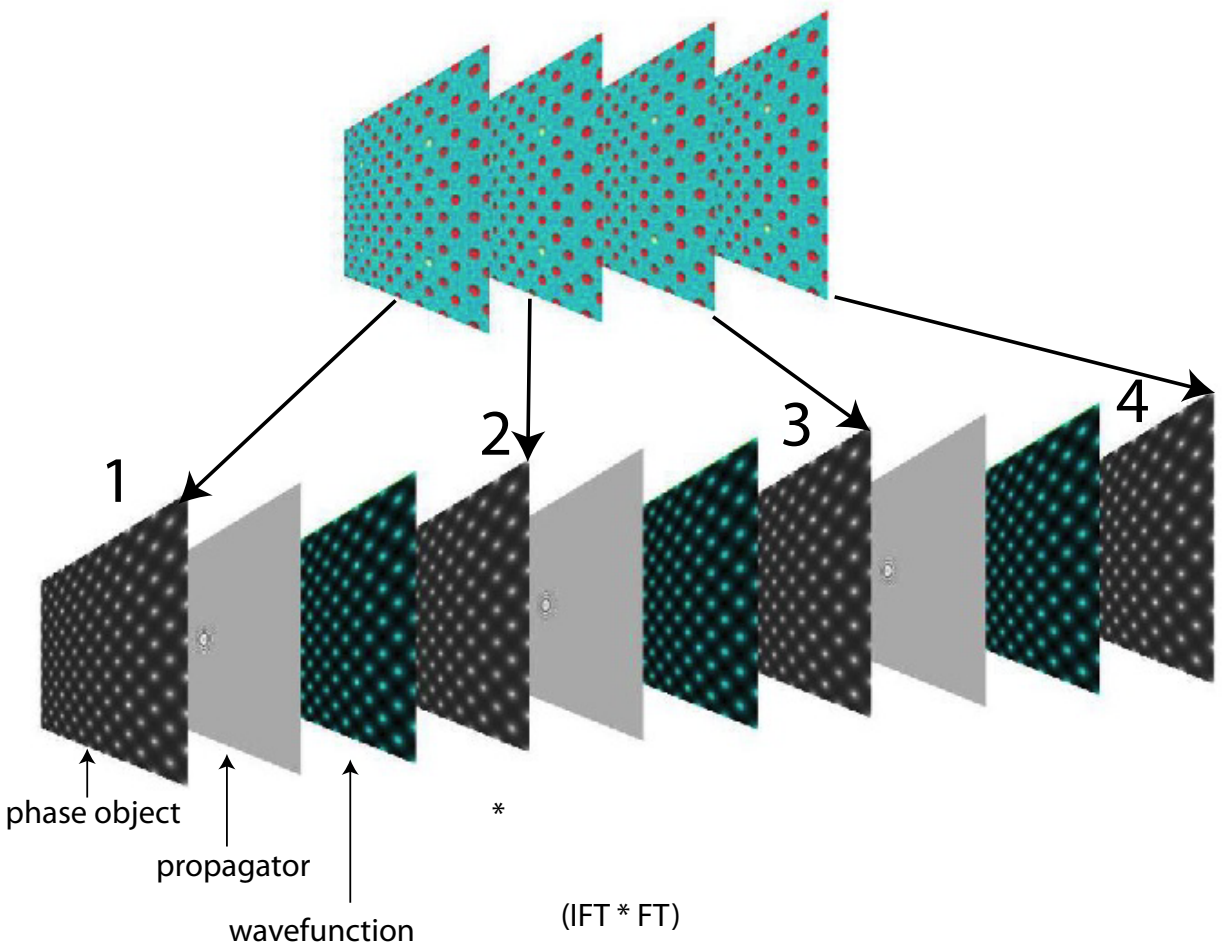

The solid is sliced into thin sub-slices. The incident wave-function is transferred by the first slice (diffraction) and propagated to the next one. The propagation is done within the Fresnel approximation, the distance between the slices being 20 - 50 times the wavelength.

$$\Psi(i+1) = [\Psi(i)PO(i)] \otimes FP_{i \to i+1}$$

Multislice algorithm

2 steps:

- Diffractor: transfer by one slice $\Rightarrow$ multiplication by phase object function ($POF(\vec{\rho})$).
- Propagator: propagation between slices $\Rightarrow$ convolution by the Fresnel propagator (is nowadays performed by a FFT followed by a multiplication and an inverse FFT (FT^{-1}, multiplication, FFT)) (calculation error $O(z)$).

For improved multislice calculations ($O(z^2)$) the wave-function is propagated over $z/2$, then multiplied by the phase-object function of the slice and finally propagated again over $z/2$. Slices do not need to have equal thicknesses.

Work best to simulate:

- Perfects crystals of large unit cell parameters[7].
- Defects under the periodic continuation assumption[8].

Is also used for:

- ADF image simulation in the "Frozen Lattice" approximation[9].

[7] K. Ishizuka, Acta Cryst. A33 (1977) 740-749.

[8] A.J. Skarnulis, Thesis, Arizona State University 1975.

[9] E.J. Kirkland, *Advanced Computing in Electron ¡microscopy.*

Multislice: periodic continuation

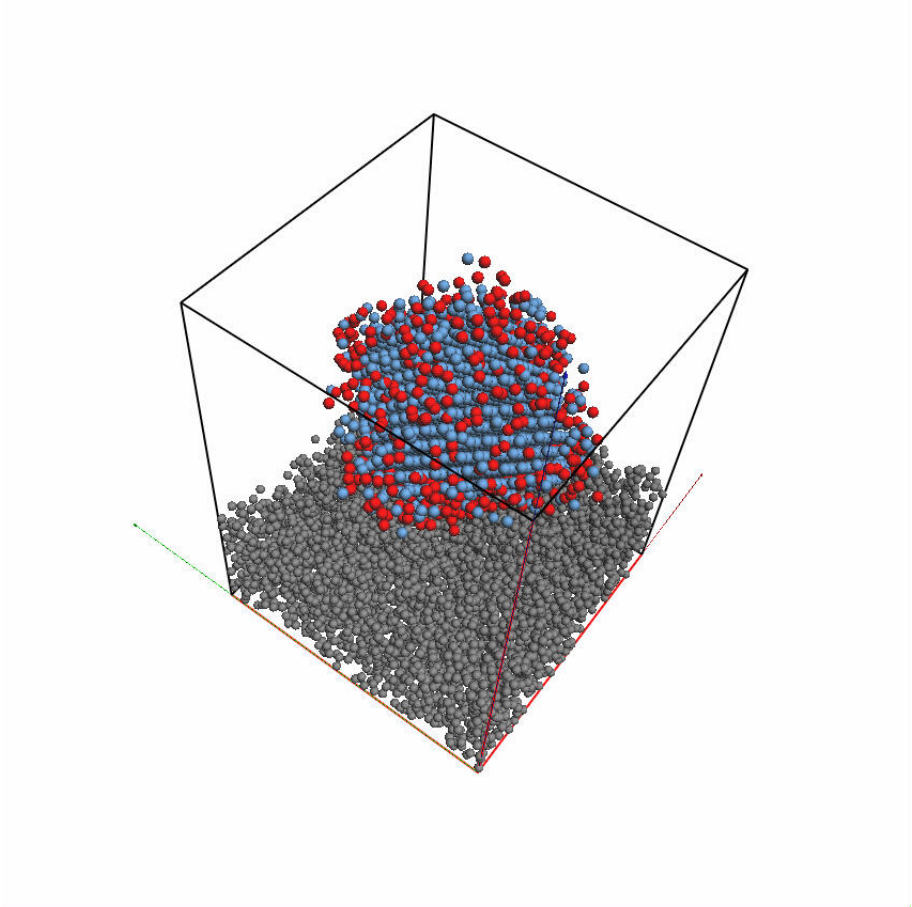

One unit cell model.

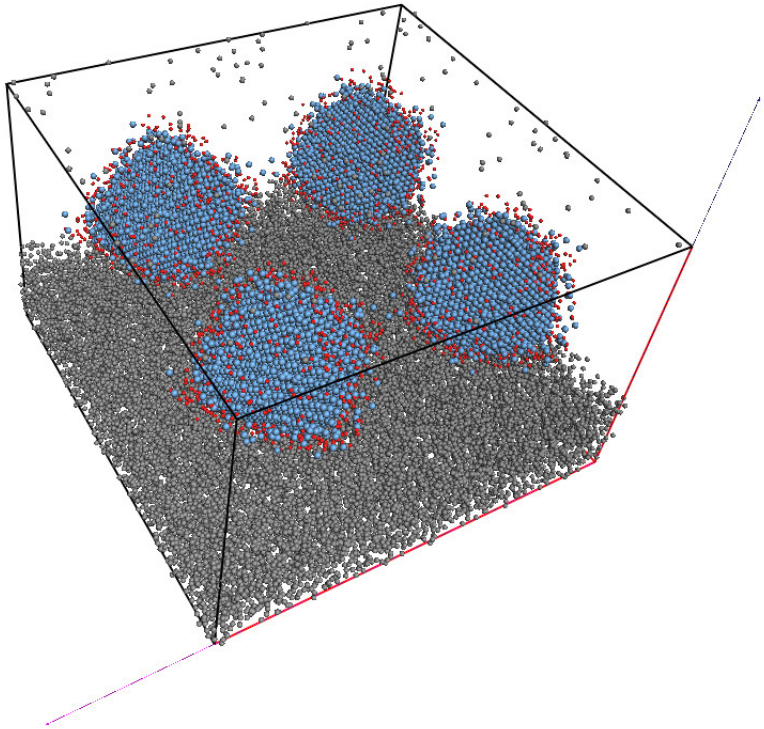

Periodic continuation model (2 x 2 unit cells).

In order to avoid "aliasing problems" during the multislice iterations the phase-object function and the propagator function must be sampled properly and also be "band-limited".

Example multislice: Pt catalyst

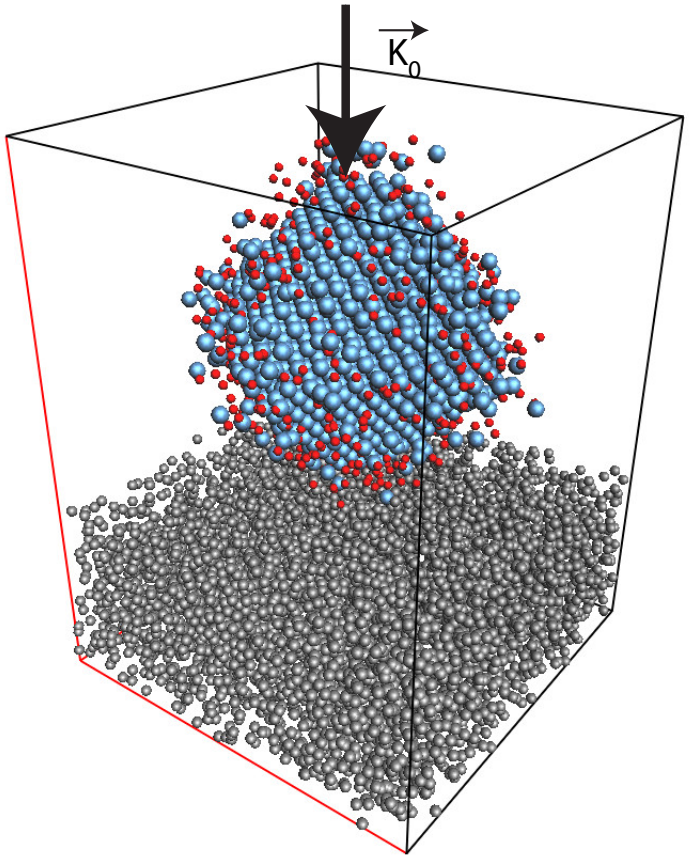

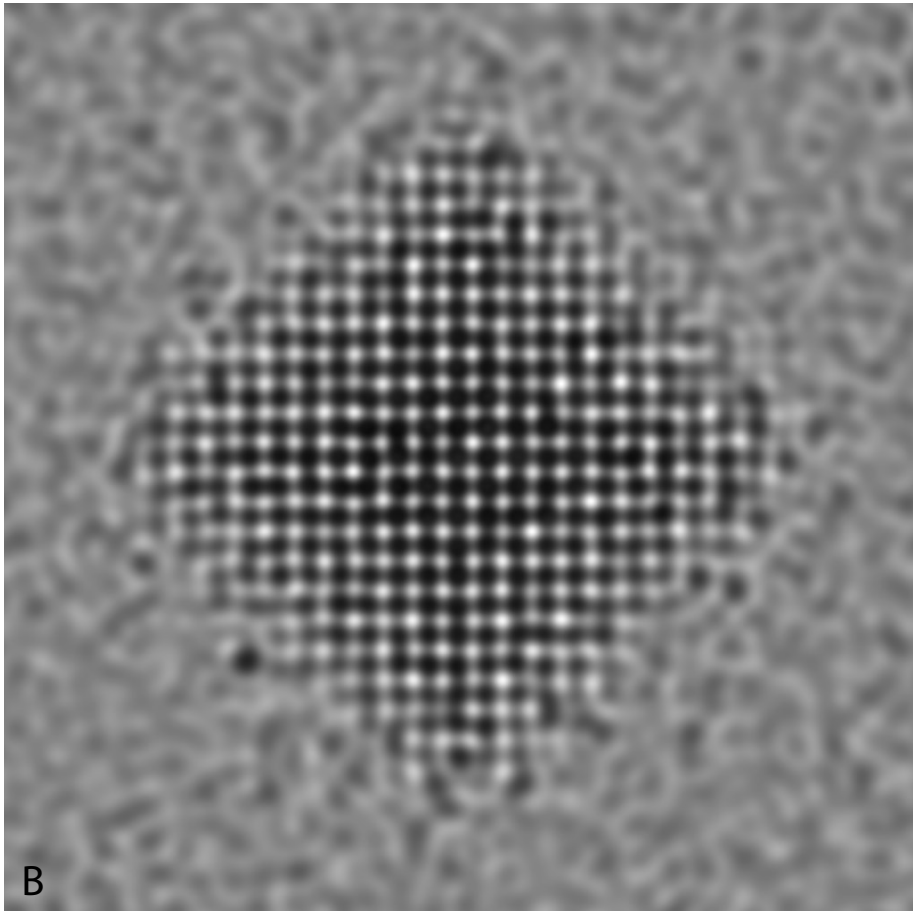

A: catalyst model (9500 atoms)

B: HREM image (Jeol 400kV).

This simulation was performed with a phase-object function sampled on a 1024 x 1024 grid.

Bloch wave method: z-independent potential

When the scattering potential is periodic, the eigenstates $|j>$ of the propagating electrons are Bloch waves. The hamiltonian of the system is projected on the eigenstates $|j>$ with eigenvalues γ_j (*"anpassung"* parameter).

$$\widehat{H} = \sum_j \gamma_j |j><j|$$

The evolution operator is then given by (since $V = V(\vec{\rho})$):

$$\widehat{U}(z,0) = e^{-i\widehat{H}z} = \sum_j e^{-i\gamma_j z}|j><j|$$

The wave-function at z developed on plane waves basis $|q>$:

$$\Psi(z) = \sum_q \phi_q(z)|q>$$

$$\phi_q(z) =< q|\widehat{U}(z,0)|0>= \sum_j e^{-i\gamma_j z} < q|j><j|0>$$

$$c_0^{*j} =< j|0> \text{ and } c_q^j =< q|j>$$

where in usual notation c_0^{*j} and c_q^j are the Bloch-wave excitations (component of the initial state $|0>$ on $|j>$) and coefficients (component of reflection $|q>$ on $|j>$) respectively[10].

[10] C. Humphreys & R.M. Fisher, Bloch Wave Notation in Many-Beam Electron Diffration, Acta Cryst. **A27** (1971) 42-45.

Bloch wave method: applications

Simulation of:

- SAED (kinematical and dynamical).
- CBED (polarity).
- LACBED (specimen thickness, symmetry).
- PED (Precession Electron Diffraction).
- HRTEM.

Works best for small lattice parameters crystals[11].

[11] Some more details in Appendix1.

CBED: ZnTe [110]

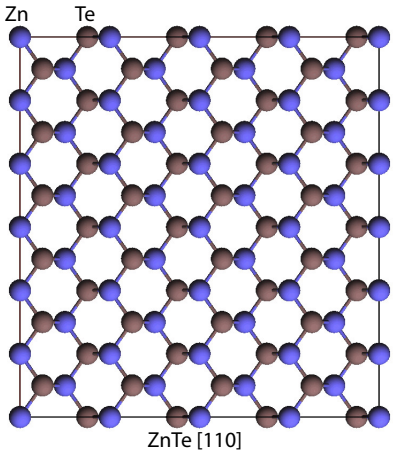

Figure : ZnTe [110].

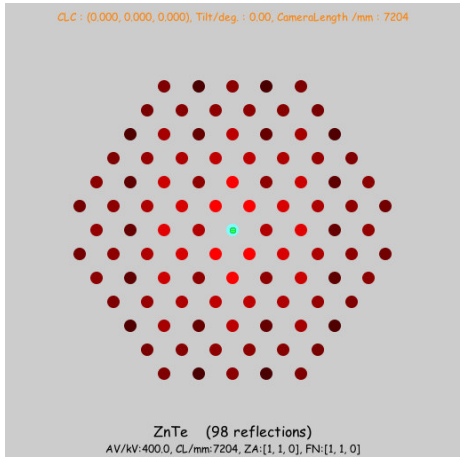

Figure : Reflections ($1 + 49$), $|\chi >= 0$.

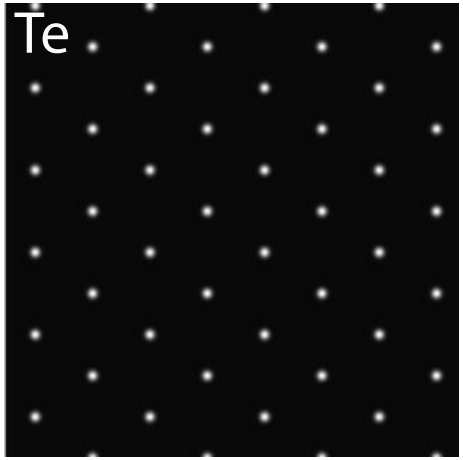

Figure : Bloch-wave 1 (Te 1s).

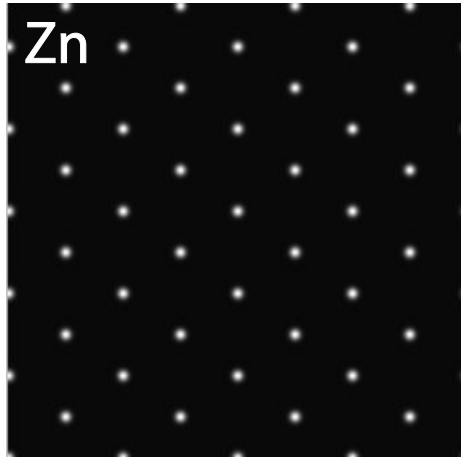

Figure : Bloch-wave 2 (Zn 1s).

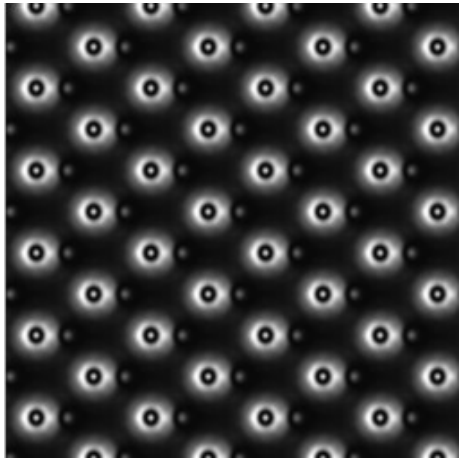

Figure : Bloch-wave 5 (Te-Zn).

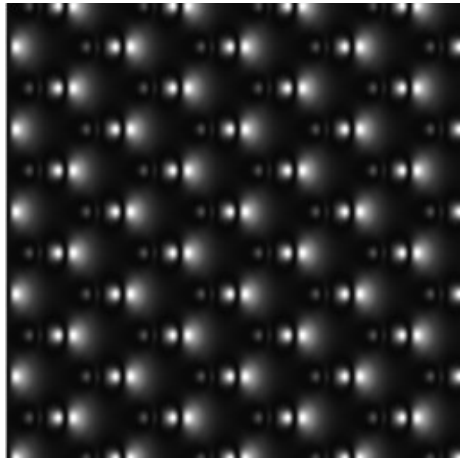

Figure : Bloch-wave 7 (Te-Zn).

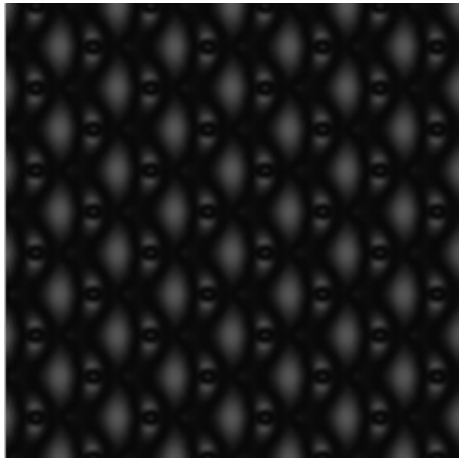

Figure : Bloch-wave 8 (Te-Zn).

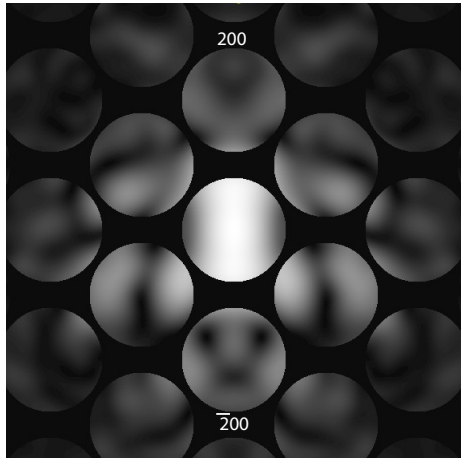

Figure : CBED (ZnTe polarity).

SAED: Diffraction pattern & specimen thickness

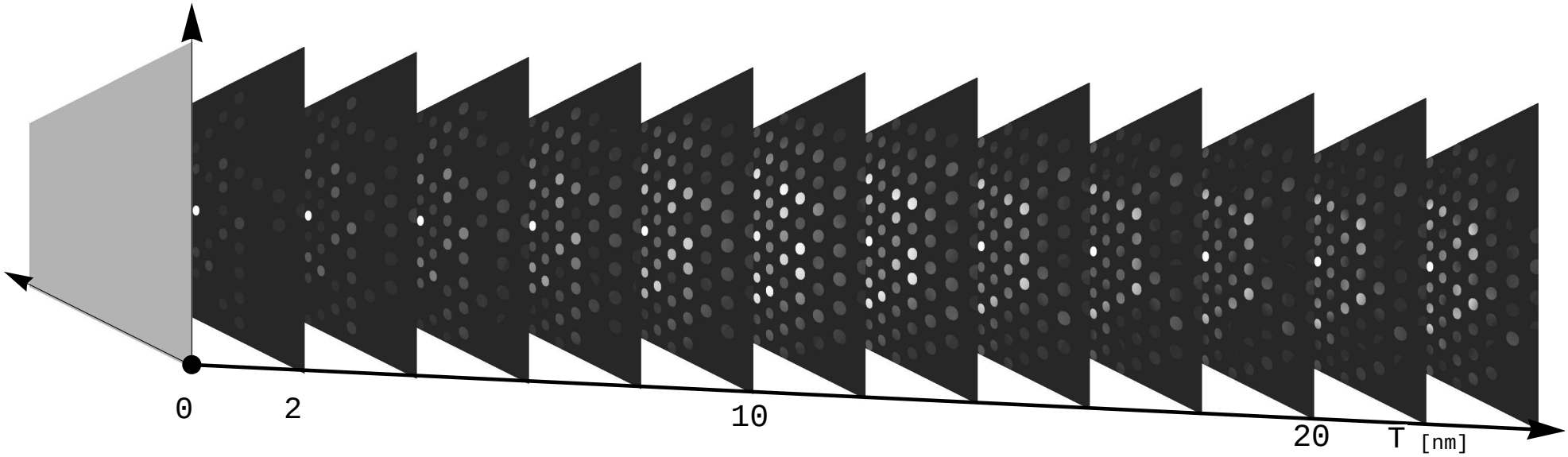

In BFP diffraction pattern depends specimen thickness.

Goodness of dynamical diffraction theories?

LACBED: Si [001]

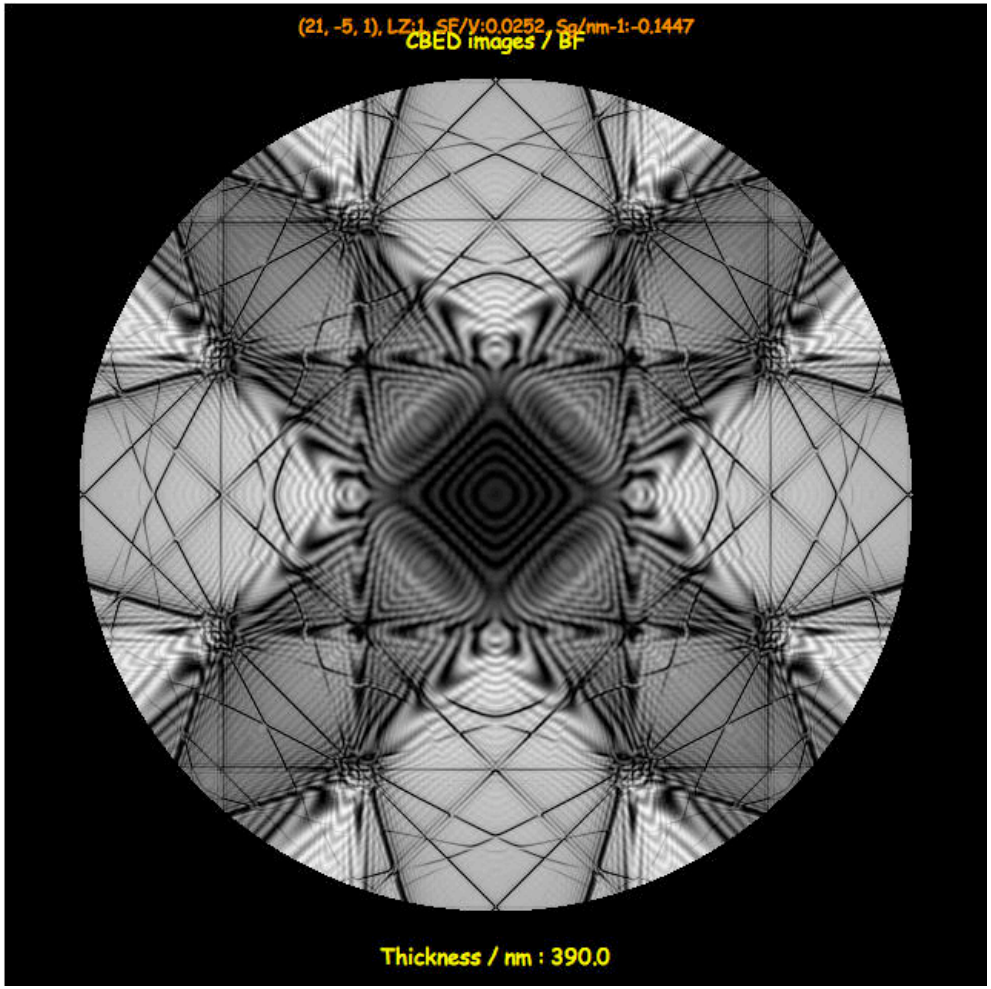

Figure : LACBED Si [001]: simulation.

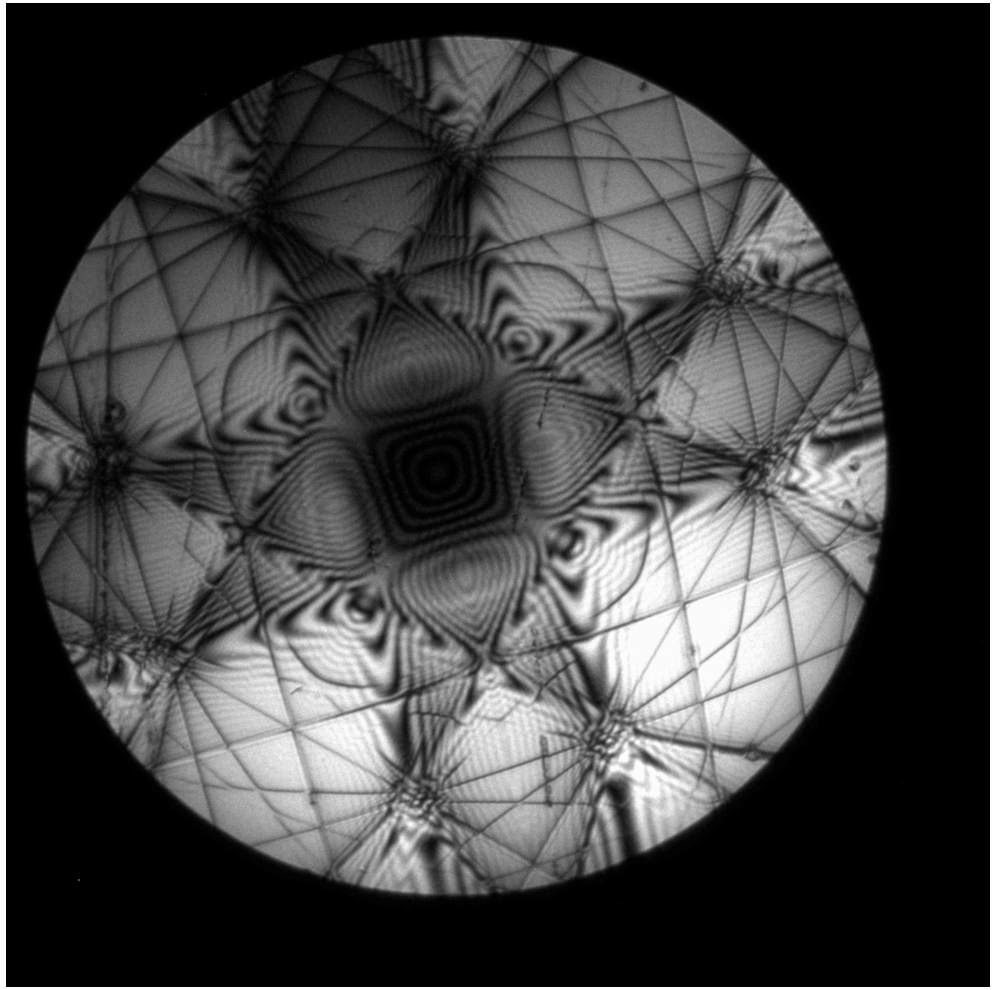

Figure : LACBED Si [001]: experimental (Web site EM centre - Monash university, J. Etheridge).

Note that the experimental LACBED pattern is blurred (inelastic scattering and/or MTF of CCD camera?).

Image formation

- Abbe image formation.
- Transfer function.
- Perfect thin lens.
- Aberrations.

Optical system

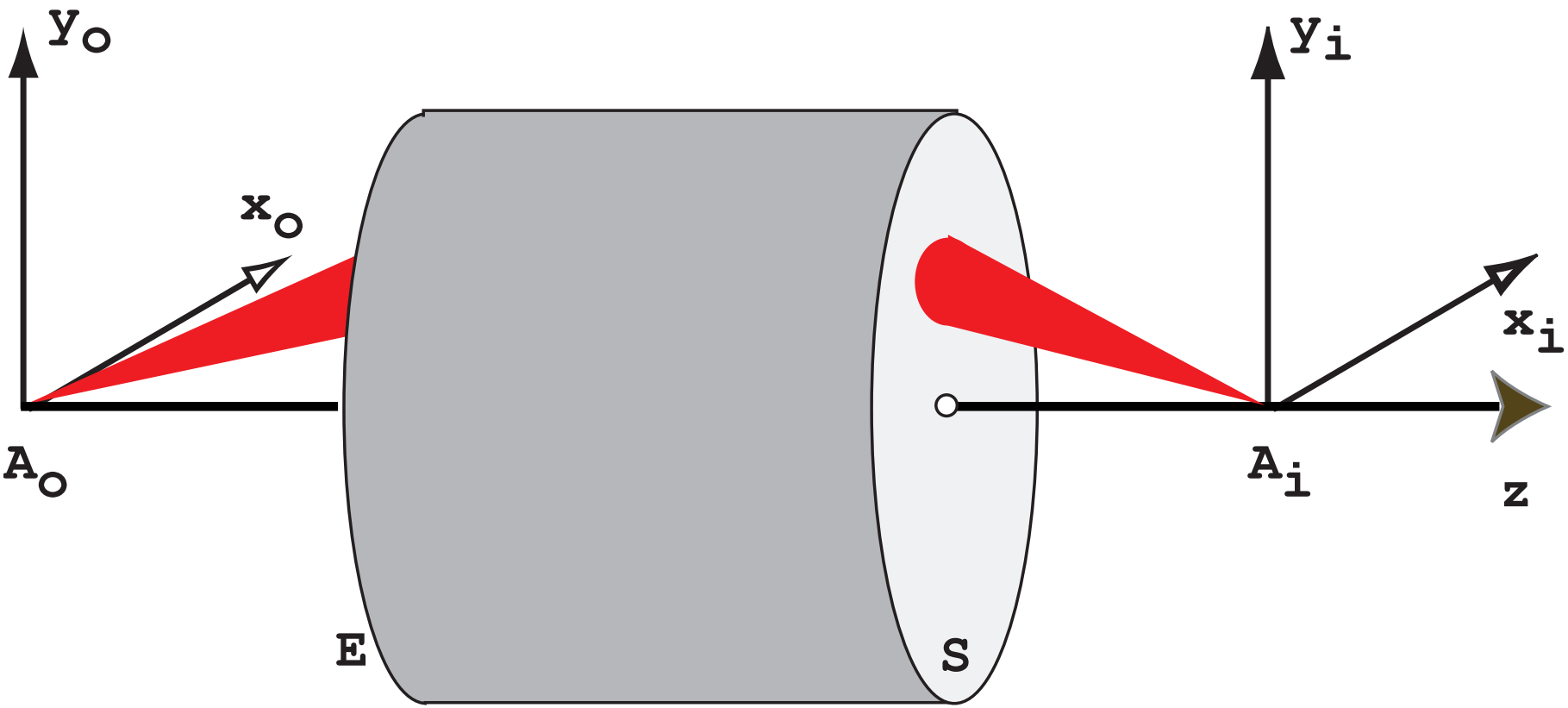

An optical system produces the image A_i of a point source object A_o. A_o and A_i are said to be conjugate. A_i is not a point since any optical system is diffraction limited. This limitation is introduced by the entrance and exit pupils of the optical system.

Aberrations of optical systems: how to define them

Some light rays emitted by object point A_o do not reach the image at point A_i.

Position of $A_i \longrightarrow$ intersection of the reference light ray (non deviated) and the image plane.

The image of a point source is a **spot** whose shape and intensity depend of the quality of the optical system.

Two types of aberrations:

1. Monochromatic.
2. Chromatic (λ dependent).

Pupils

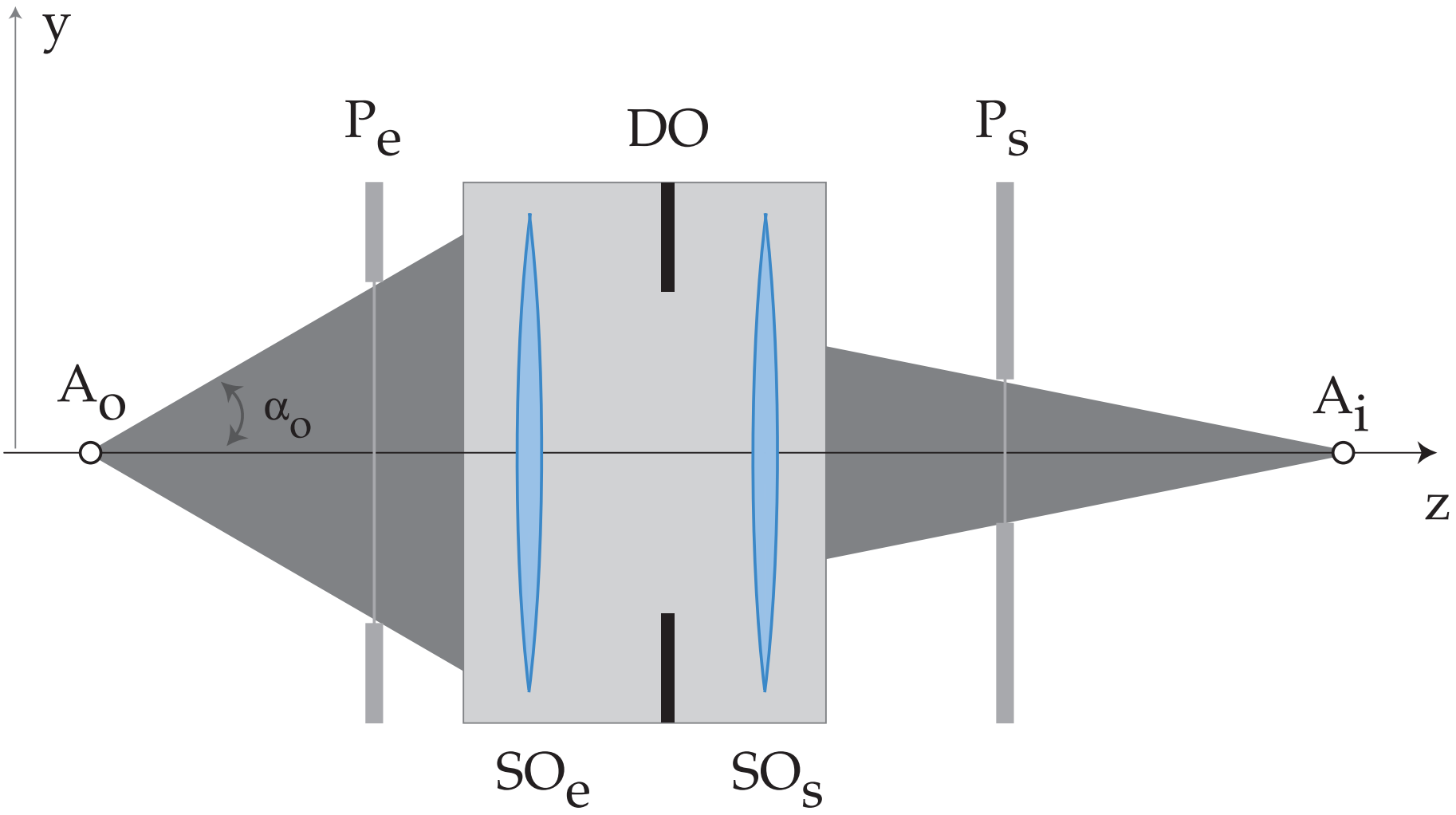

Any optical system can be characterised by an entrance pupil P_e and an exit pupil P_s. The pupils are the image of the opening aperture DO by the entrance and exit optical subsystems SO_e and SO_s. What are P_e and P_s for a thin lens?

Monochromatic aberrations

In order to evaluate the monochromatic aberrations one must define a function characteristic of the optical system.

This function will depend on:

1. The selected reference planes.
2. The optical path followed by the light ray.

Optical Path Length: OPL

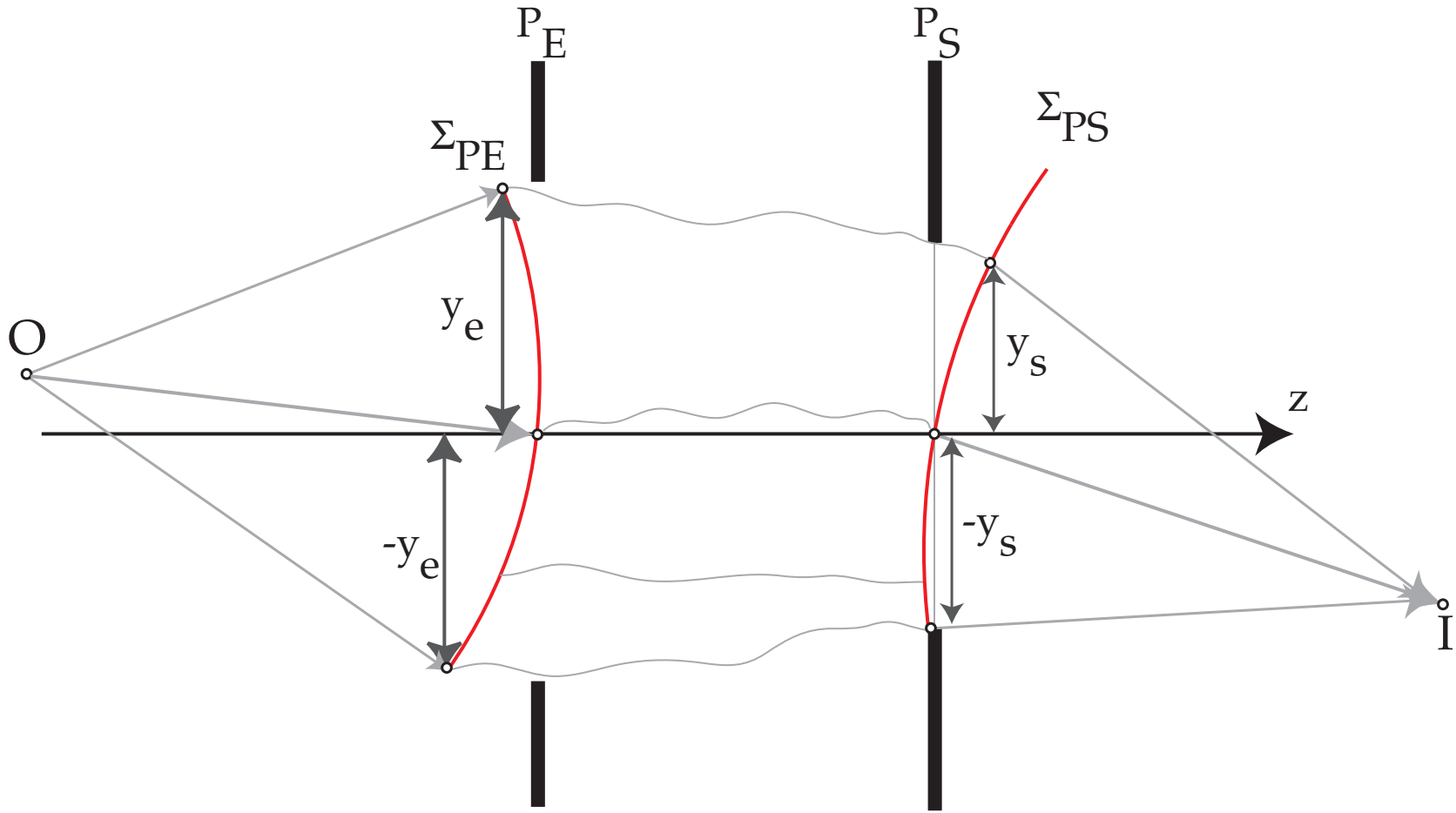

- Before P_E the reference wavefront Σ_{PE} is spherical (point source at O).
- After P_S the reference wavefront Σ_{PS} is spherical (converges towards I).

For a perfect optical system, both the entrance Σ_{PE} and exit Σ_{PS} wavefronts are spherical. The Optical Path Length form O to I is independent of the path.

Optical Path Difference (OPD): aberrations

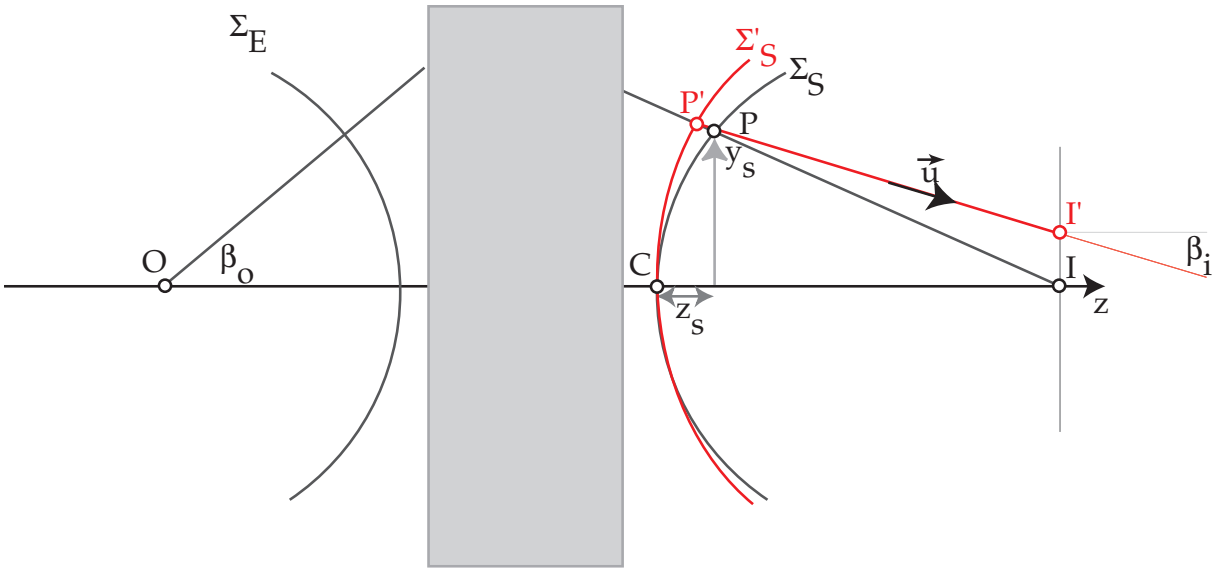

In the presence of aberrations the wavefront Σ'_S is no more spherical. The Optical Path Difference (distance between the deformed Σ'_S and spherical wavefront Σ_S) introduces a phase shift $\delta\phi$. With P' close to $P = (x_s, y_s)$ on reference sphere Σ_s, the OPD at $P' =$ (i.e. OPL from P' to P) is given by (Fermat principle):

$$W(x_s, y_s) = n_i \overline{P'P}$$

n_i refractive index of the medium $\longrightarrow$ phase shift:

$$\delta\phi = e^{2\pi\imath \frac{W(x_s, y_s)}{\lambda}}$$

Transverse geometric aberrations: $\vec{\epsilon}$

The transverse geometric aberrations are proportional to $\frac{d}{d\theta}$ wavefront aberrations[12]:

$$\epsilon_x = -\frac{f}{n_i}\frac{\partial W}{\partial x_s}$$
$$\epsilon_y = -\frac{f}{n_i}\frac{\partial W}{\partial y_s}$$

f focal length.

The OPD's introduced by all the aberrations of the imaging system are collected in a function $\chi(\vec{u})$ and the phase shift is[13]:

$$\widetilde{T}(\vec{u}) = e^{\imath\chi(\vec{u})}$$

$\widetilde{T}(\vec{u})$ has been first employed by Abbe in his description of image formation (1866).

[12] $P(x_s, y_s)$ on the spherical reference wavefront can be characterised by the radial angle θ.

[13] The angle θ corresponds (through Bragg law) to a spatial frequency $\vec{u}$, i.e. a distance in the back focal plane.

Paraxial optics: principal rays

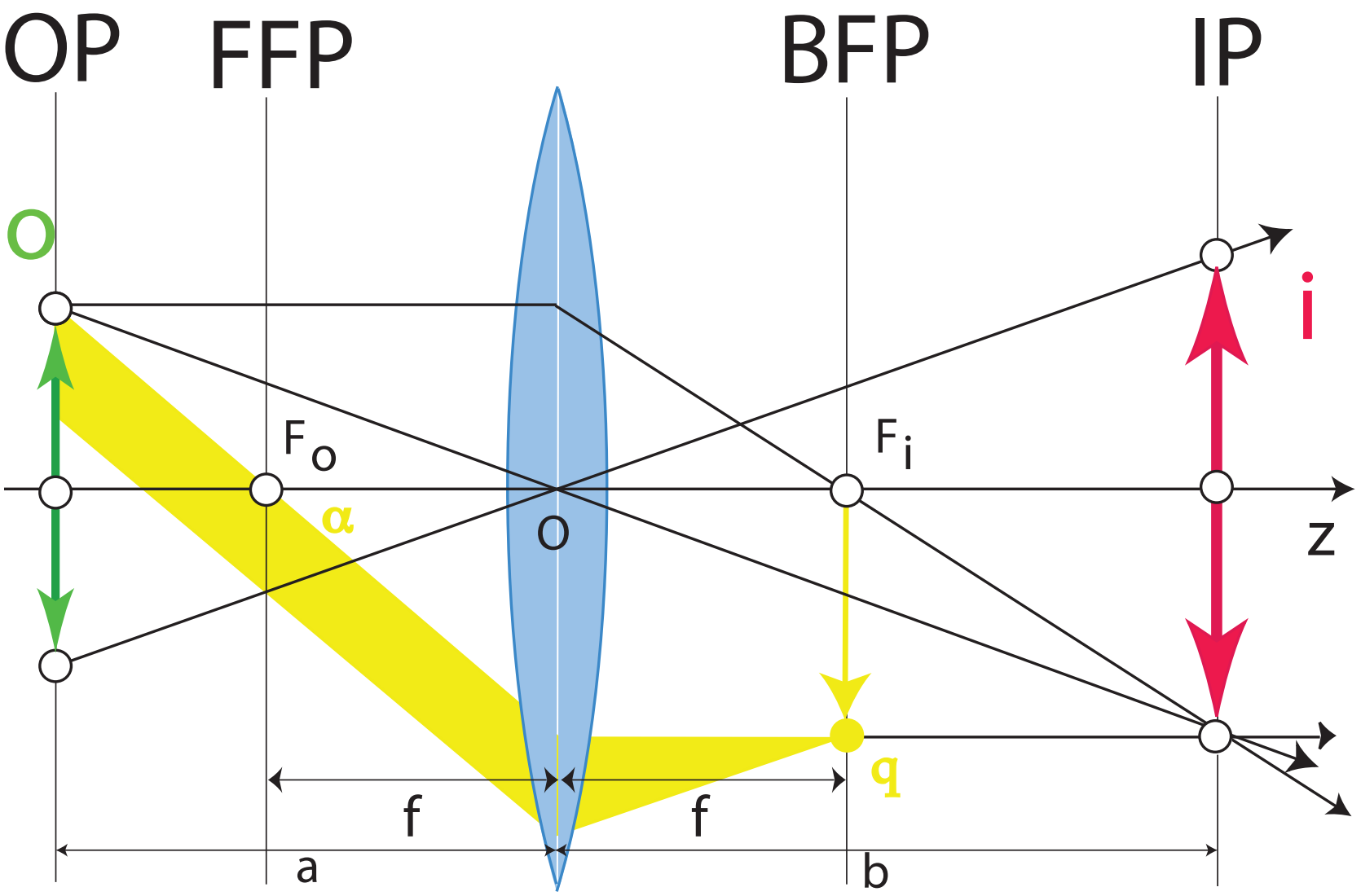

Principal rays of paraxial optics. Reflection (plane wave) making an angle α, where $\alpha = 2\theta_B$, corresponds to spatial frequency u.

Microscope modelling: Abbe image formation theory

Objective lens is modelled as a thin lens that brings Fraunhofer diffraction pattern at finite distance (i.e. in its Back Focal Plane).

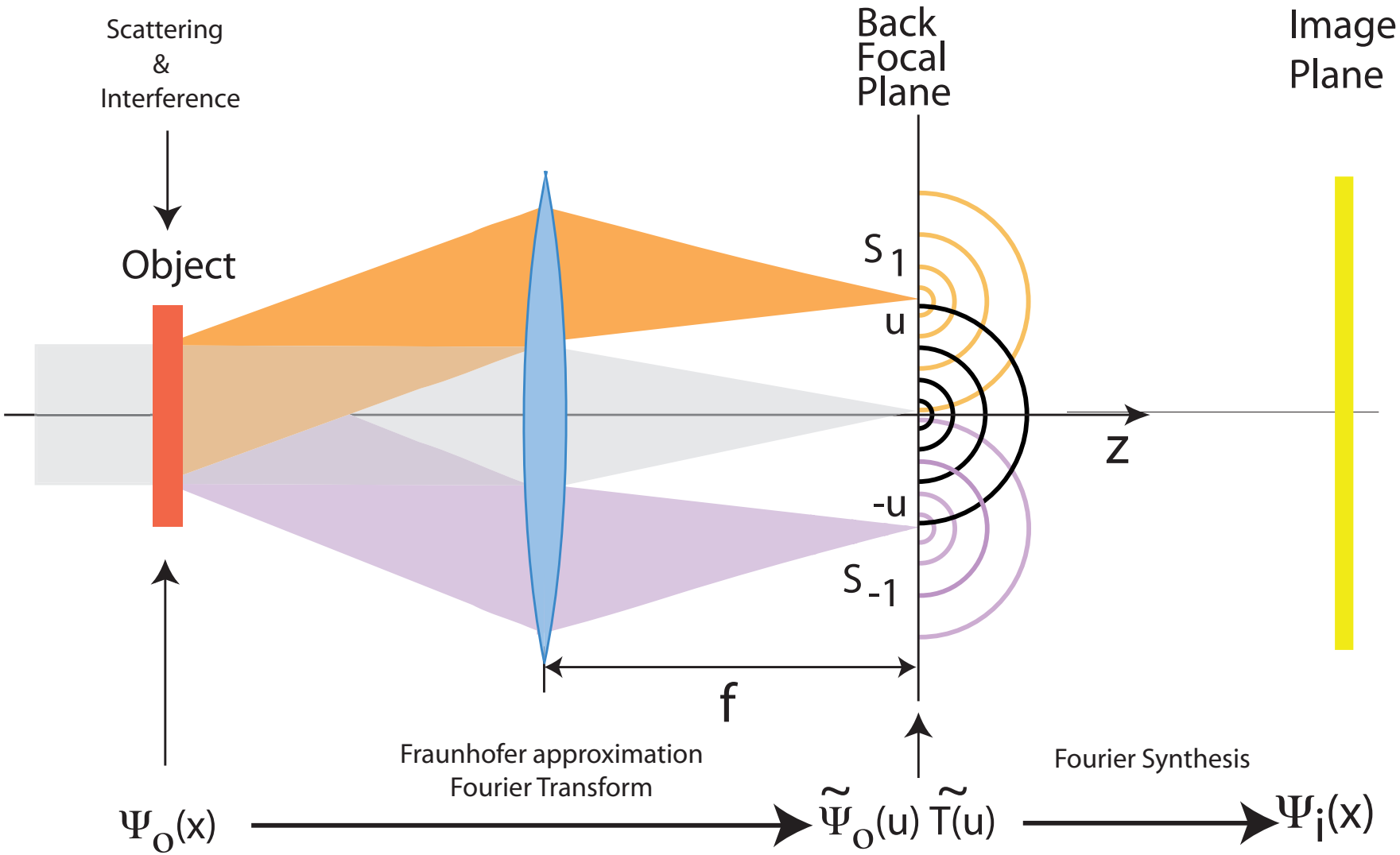

Transfer by objective lens: $< q' | \widetilde{T}(q', q) | q >$

Image forming system has 2 properties (Abbe theory):

- Linear.
- Space invariant.

Coherence of illumination:

- Source size (spatial coherence).
- Energy spread (temporal coherence).

Partial coherence (always the case): $\widetilde{T}(q', q)$: transmission cross-coefficients $\Longrightarrow$ is approximated by a transfer function $\widetilde{T}(\vec{u})$ and several envelope functions (attenuation of a range of spatial frequencies)..

Transfer Function $\widetilde{T}(\vec{u})$ and Optical Transfer Function $\widetilde{OTF}(\vec{u})$

Two cases:

$\rightarrow$ **TEM** ($\widetilde{T}(\vec{u})$: Transfer Function):

$$\begin{aligned}\widetilde{\Psi}_i(\vec{u}) &= \widetilde{\Psi}_o(\vec{u})\widetilde{T}(\vec{u}) \\ \Psi_i(\vec{x}) &= \int \widetilde{\Psi}_o(\vec{u})\widetilde{T}(\vec{u})e^{2\pi\imath\vec{u}\cdot\vec{x}}\mathrm{d}\vec{u}\end{aligned}$$

$\rightarrow$ **STEM** ($\widetilde{OTF}(\vec{u}) = \widetilde{T}(\vec{u}) \otimes \widetilde{T}(-\vec{u})$: Optical Transfer Function):

$$\begin{aligned}
I(\vec{x}) &= \langle \Psi_i(\vec{x};t)\Psi_i^*(\vec{x};t)\rangle \\
\Psi_i(\vec{x};t) &= \Psi_o(\vec{x};t) \otimes T(\vec{x}) \\
I(\vec{x}) &= \langle [\Psi_o(\vec{x};t) \otimes T(\vec{x})][\Psi_o^*(\vec{x};t) \otimes T^*(\vec{x})]\rangle && (\otimes \text{ convolution.}) \\
I(\vec{x}) &= [T(\vec{x})T^*(\vec{x})] \otimes \langle \Psi_o(\vec{x};t)\Psi_o^*(\vec{x};t)\rangle && (T(\vec{x}) \text{ is time independent.}) \\
\langle \Psi_o(\vec{x};t)\Psi_o^*(\vec{x};t)\rangle &= |\Psi_o(\vec{x})|^2 && (\text{complete spatial incoherence}) \\
I(\vec{x}) &= |\Psi_o(\vec{x})|^2 \otimes [T(\vec{x})T^*(\vec{x})] \\
I(\vec{x}) &= I_o(\vec{x}) \otimes OTF(\vec{x})
\end{aligned}$$

Optical Path Length: underfocus

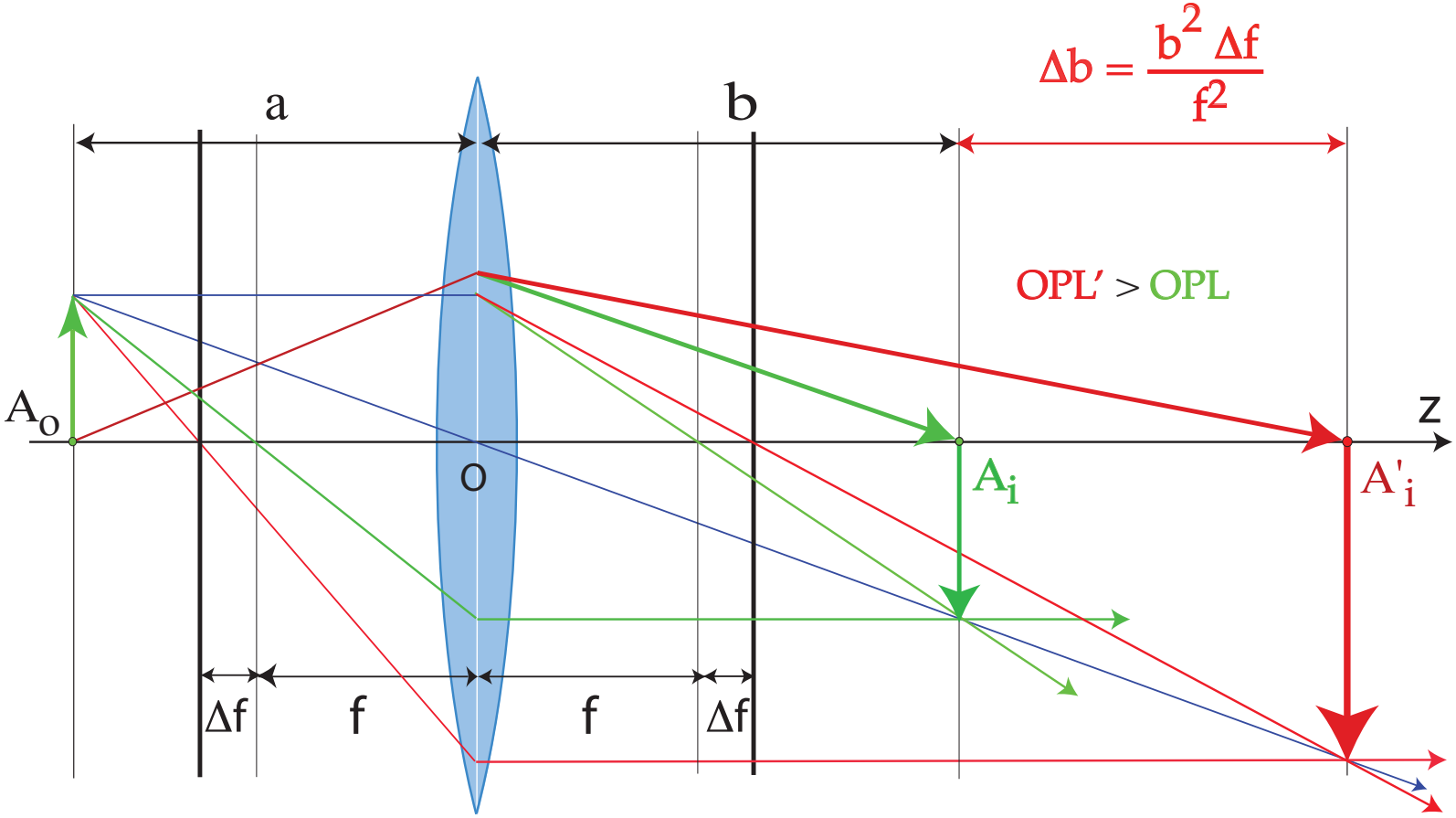

Underfocus weakens the objective lens, i.e. increases f. As a consequence the OPL from A_o to A'_i is larger:

$$e^{2\pi i \frac{\Delta f \lambda (\vec{q} \cdot \vec{q})}{2}}$$

Transfer function $T(\vec{q})$

$$T(\vec{q}) = e^{i\chi(\vec{q})} = \cos(\chi(\vec{q})) + i \underbrace{\sin(\chi(\vec{q}))}_{\text{Contrast transfer function}}$$

$$\chi(\vec{q}) = \pi \left[W_{20}\, \lambda\, \vec{q}.\vec{q} + W_{40} \frac{\lambda^3 (\vec{q}.\vec{q})^2}{2} + ... \right]$$

Where:

- W_{20} : defocus (z)
- W_{40}: spherical aberration (C_s)

Wave-front aberrations to 6^{th} order (cartesian coordinates)

$\{z, \pi\,(u^2+v^2)\,\lambda\}$ (*defocus*)
$\{W(1,1), 2\pi(u\cos(\phi(1,1)) + v\sin(\phi(1,1)))\}$
$\{W(2,2), \pi\lambda((u-v)(u+v)\cos(2\phi(2,2)) + 2uv\sin(2\phi(2,2)))\}$
$\left\{W(3,1), \frac{2}{3}\pi\,(u^2+v^2)\,\lambda^2(u\cos(\phi(3,1)) + v\sin(\phi(3,1)))\right\}$
$\left\{W(3,3), \frac{2}{3}\pi\lambda^2\,(u\,(u^2-3v^2)\cos(3\phi(3,3)) - v\,(v^2-3u^2)\sin(3\phi(3,3)))\right\}$
$\left\{W(4,0), \frac{1}{2}\pi\,(u^2+v^2)^2\,\lambda^3\right\}$ (3^{rd} *order spherical aberration or* C_3)
$\left\{W(4,2), \frac{1}{2}\pi\,(u^2+v^2)\,\lambda^3((u-v)(u+v)\cos(2\phi(4,2)) + 2uv\sin(2\phi(4,2)))\right\}$
$\left\{W(4,4), \frac{1}{2}\pi\lambda^3\,((u^4-6v^2u^2+v^4)\cos(4\phi(4,4)) + 4u(u-v)v(u+v)\sin(4\phi(4,4)))\right\}$
$\left\{W(5,1), \frac{2}{5}\pi\,(u^2+v^2)^2\,\lambda^4(u\cos(\phi(5,1)) + v\sin(\phi(5,1)))\right\}$
$\left\{W(5,3), \frac{2}{5}\pi\,(u^2+v^2)\,\lambda^4\,(u\,(u^2-3v^2)\cos(3\phi(5,3)) - v\,(v^2-3u^2)\sin(3\phi(5,3)))\right\}$
$\left\{W(5,5), \frac{2}{5}\pi\lambda^4\,(u\,(u^4-10v^2u^2+5v^4)\cos(5\phi(5,5)) + v\,(5u^4-10v^2u^2+v^4)\sin(5\phi(5,5)))\right\}$
$\left\{W(6,0), \frac{1}{3}\pi\,(u^2+v^2)^3\,\lambda^5\right\}$ (5^{th} *order spherical aberration or* C_5)
$\left\{W(6,2), \frac{1}{3}\pi\,(u^2+v^2)^2\,\lambda^5((u-v)(u+v)\cos(2\phi(6,2)) + 2uv\sin(2\phi(6,2)))\right\}$
$\left\{W(6,4), \frac{1}{3}\pi\lambda^5\,((u^6-5v^2u^4-5v^4u^2+v^6)\cos(4\phi(6,4)) + 4uv\,(u^4-v^4)\sin(4\phi(6,4)))\right\}$
$\left\{W(6,6), \frac{1}{3}\pi\lambda^5\,((u^6-15v^2u^4+15v^4u^2-v^6)\cos(6\phi(6,6)) + 2uv\,(3u^4-10v^2u^2+3v^4)\sin(6\phi(6,6)))\right\}$

jems describes wave-front aberrations to order 8.

Wave-front aberrations to order 8

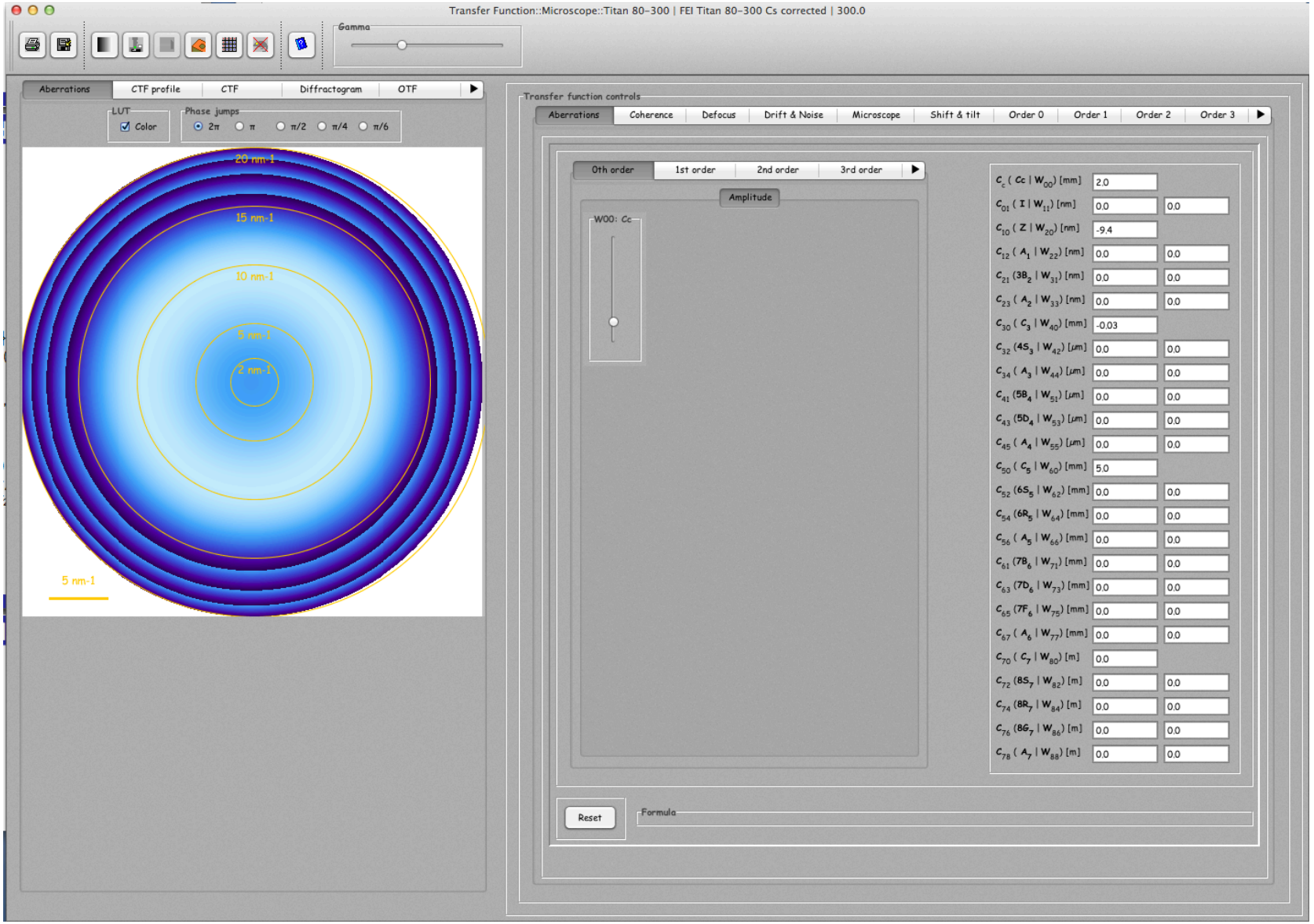

Contrast transfer function: $\sin(\chi(\vec{q}))$

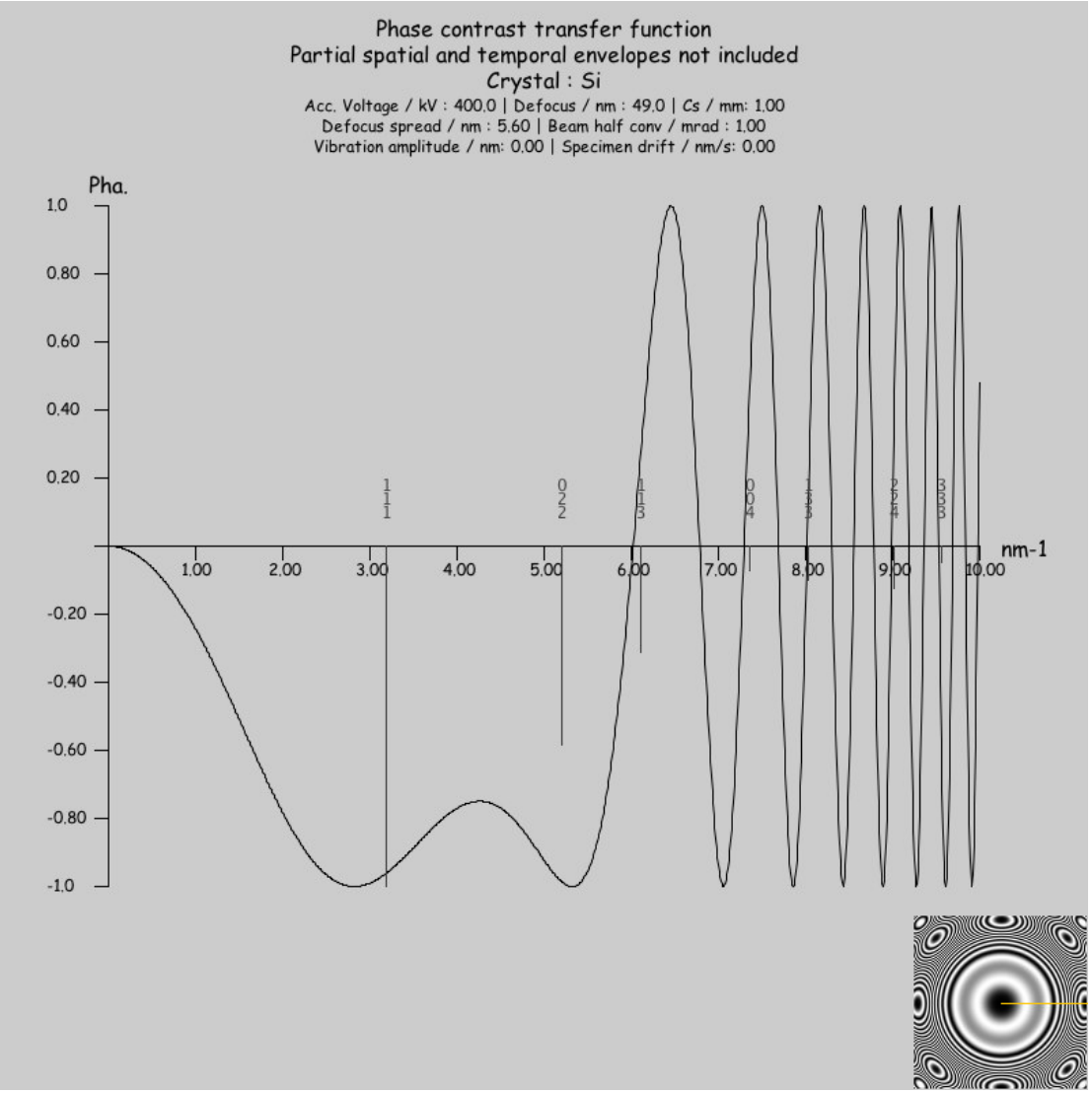

The transfer function of the objective lens in the absence of lens current and accelerating voltage fluctuations (Scherzer defocus). The (111) and (022) reflections of Si are phase shifted by $-\frac{\pi}{2} \rightarrow$ black atomic columns.

HRTEM image intensity: WPOA

In the Weak Phase Object Approximation under optimum transfer conditions the image intensity $I(\vec{x})$ is:

- positive C_s (black atomic columns)

$$I(\vec{x}) \sim 1 - 2\sigma V_p(\vec{x})$$

- negative C_s (white atomic columns)

$$I(\vec{x}) \sim \sigma V_p(\vec{x})$$

Where:

$$V_p(\vec{x}) : \text{projected potential}$$

$$\sigma : \text{electron matter interaction constant}$$

HRTEM image depends on specimen thickness and object defocus

Thickness series

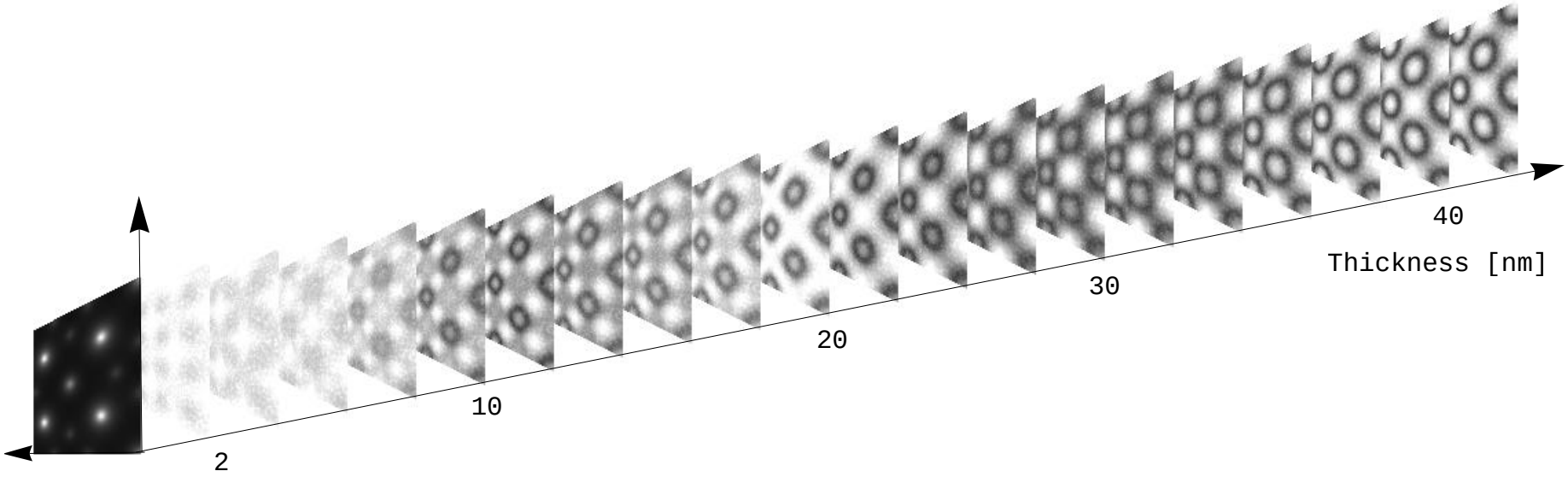

Defocus series

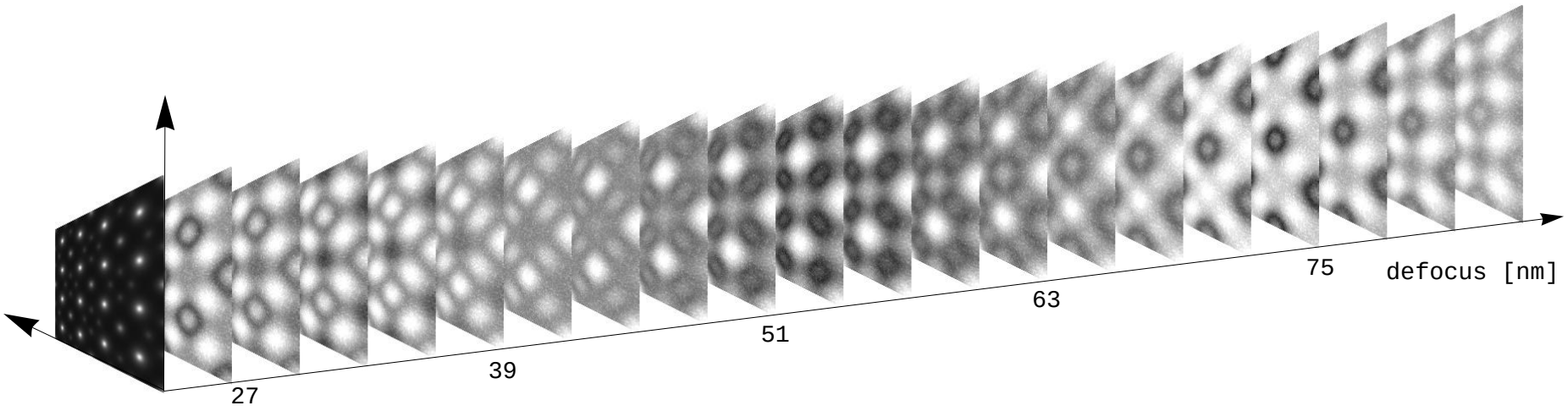

Si [001] images map: contrast dependence of defocus & thickness

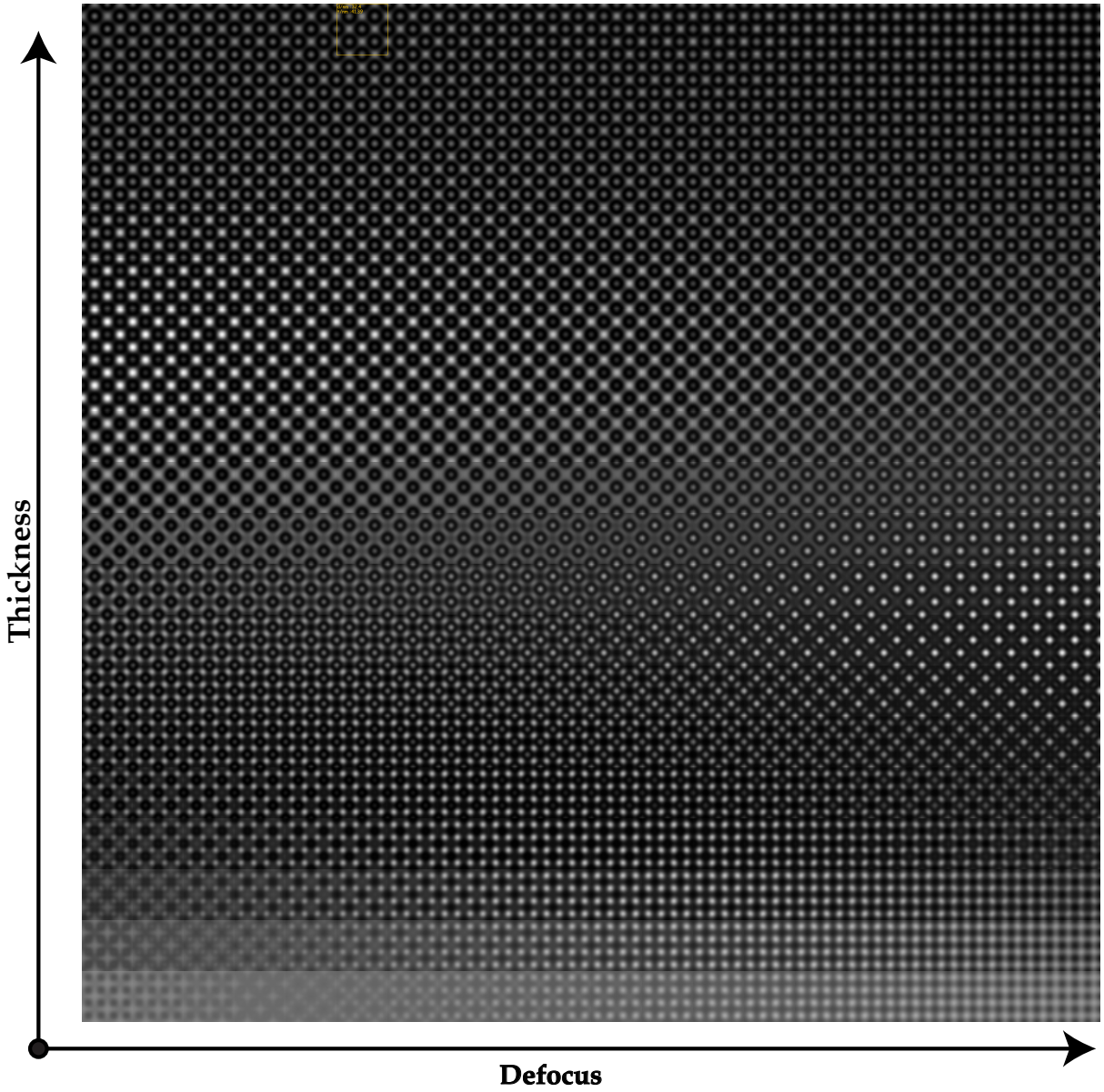

HREM map does not include the Modulation Transfer Function (MTF) of the detector.

Problems

Problems...

- Object
  - $\rightarrow$ Atomic scattering amplitude below 50 kV?
  - $\rightarrow$ Potential by DFT calculation?
  - ...
- HRTEM $\rightarrow$ Phase of diffracted beams evolves with specimen thickness.
- HRTEM $\rightarrow$ MTF of image acquisition system (Stobbs factor?).
- HRTEM / HRSTEM $\rightarrow$ Electron channeling depends on atomic column content.
- HRTEM / HRSTEM $\rightarrow$ Aberrations of optical system.
- HRTEM $\rightarrow$ Inelastic scattering (J.M. Cowley, E.J. Kirkland, D. van Dyck, A. Rosenaurer, K. Ishizuka, Z.L. Wang, H. Rose, H. Mueller, L. Allen, ...).
- HRTEM / HRSTEM $\rightarrow$ Drift, vibration, Johnson-Nyquist noise[14], ...
- ...

[14] S. Uhlemann, H. Mueller, P. Hartel, J. Zach & M. Haider, Phys. Rev. Lett. **111** (2013) 046101.

HRTEM problem: amplitude and phase of diffracted beams

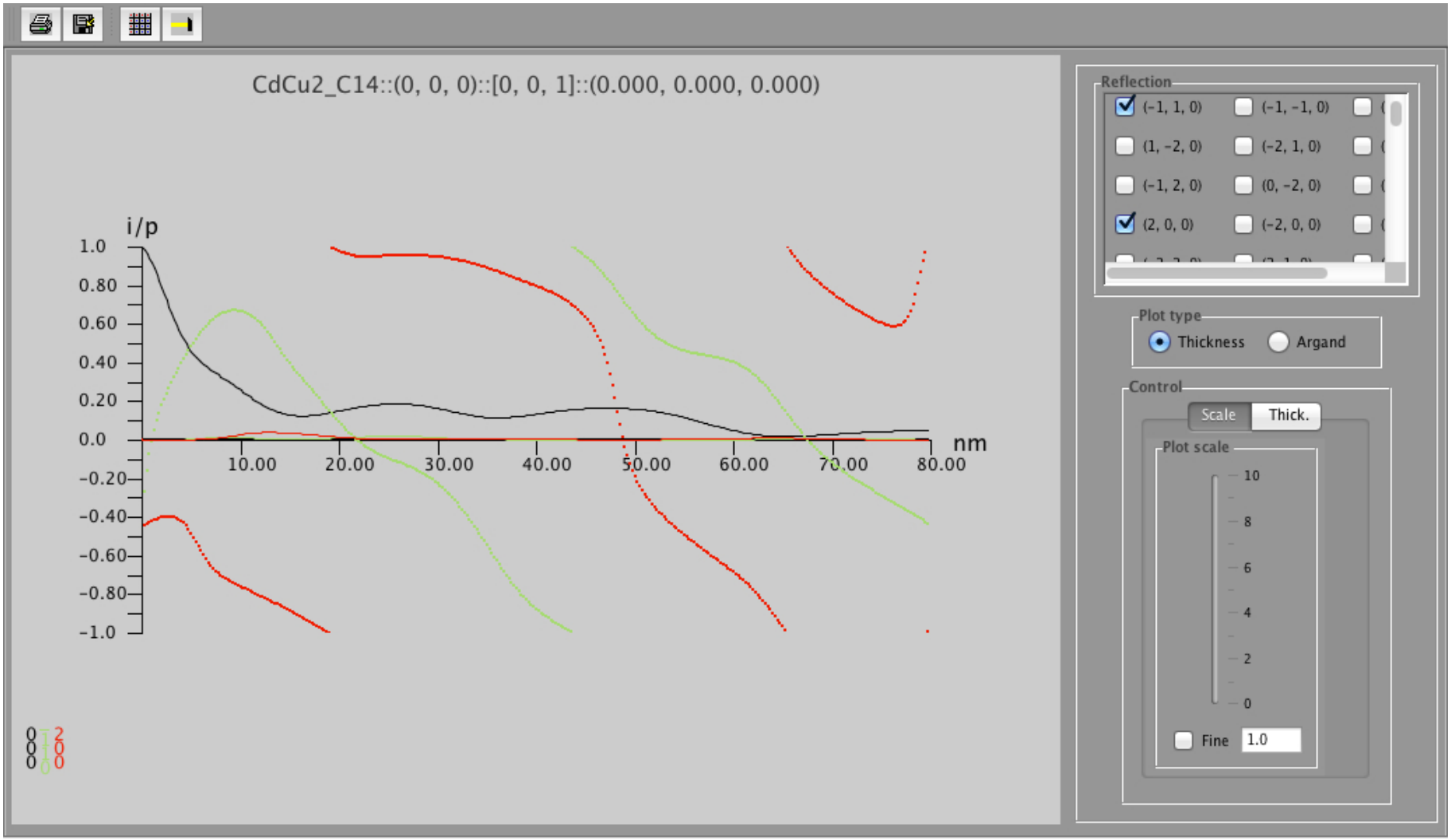

Note that phase of diffracted beam is $\frac{\pi}{2}$ out-of-phase with respect to transmitted beam.

HRTEM problem: CCD MTF (Gatan MSC 1K x 1K, 24 μm)

To make quantitative comparison with experimental HRTEM images the MTF of the detector must be introduced in the simulation.

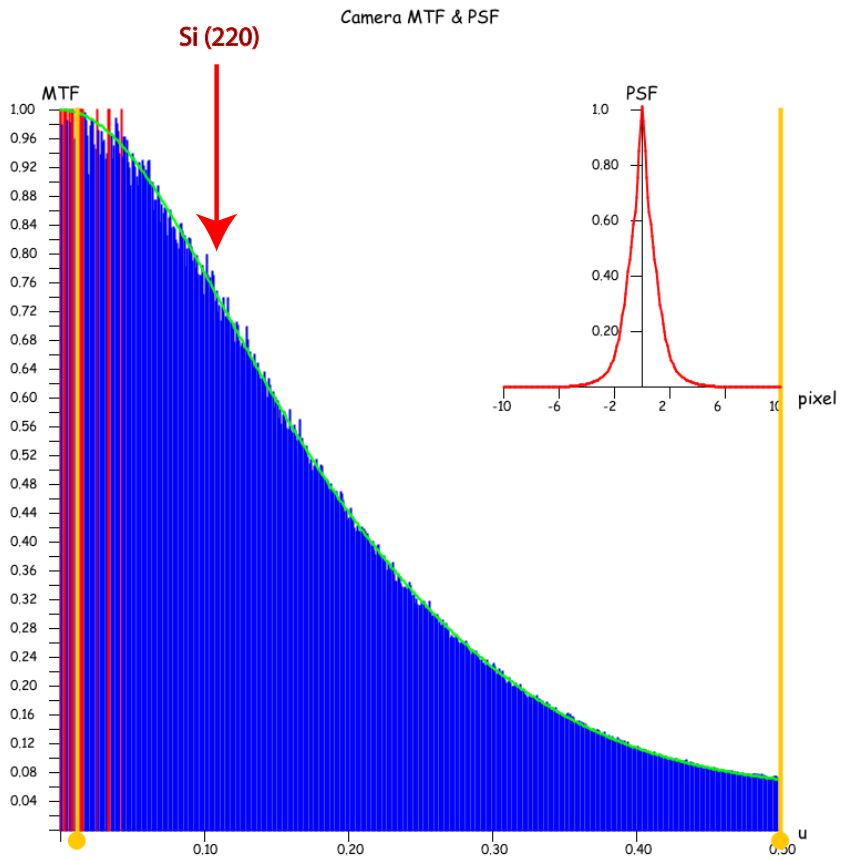

Figure : At high magnification Si (220) planes imaged with high contrast.

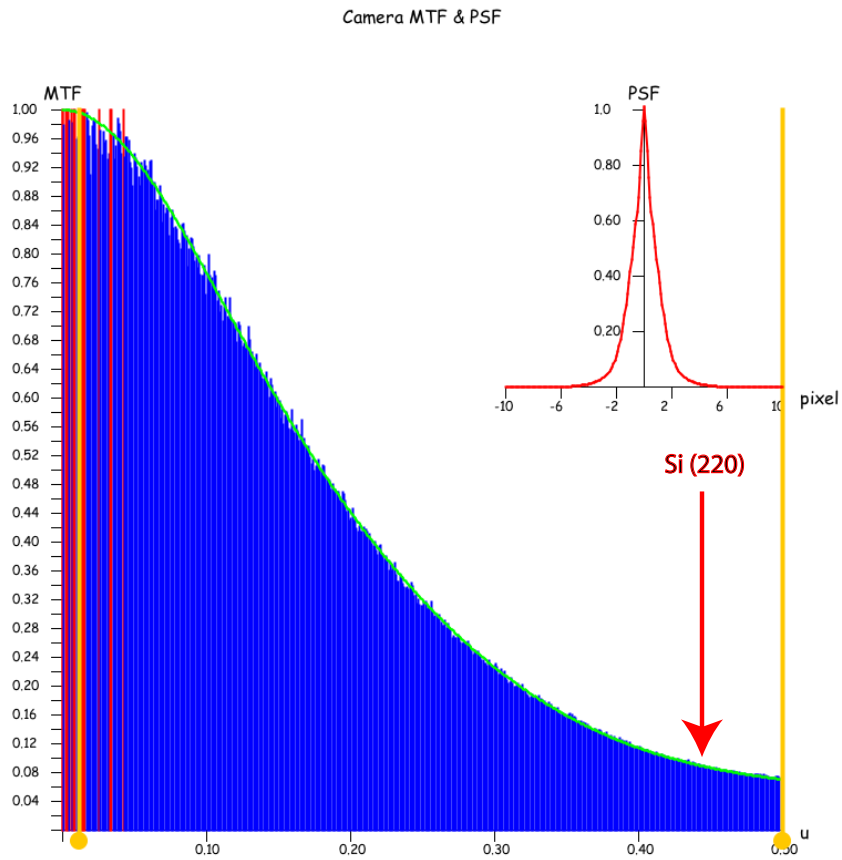

Figure : At low magnification Si (220) planes imaged with low contrast.

For quantitative comparison always use highest possible magnification (or include CCD MTF in simulations)!

CCD MTF: high magnification (900 kx)

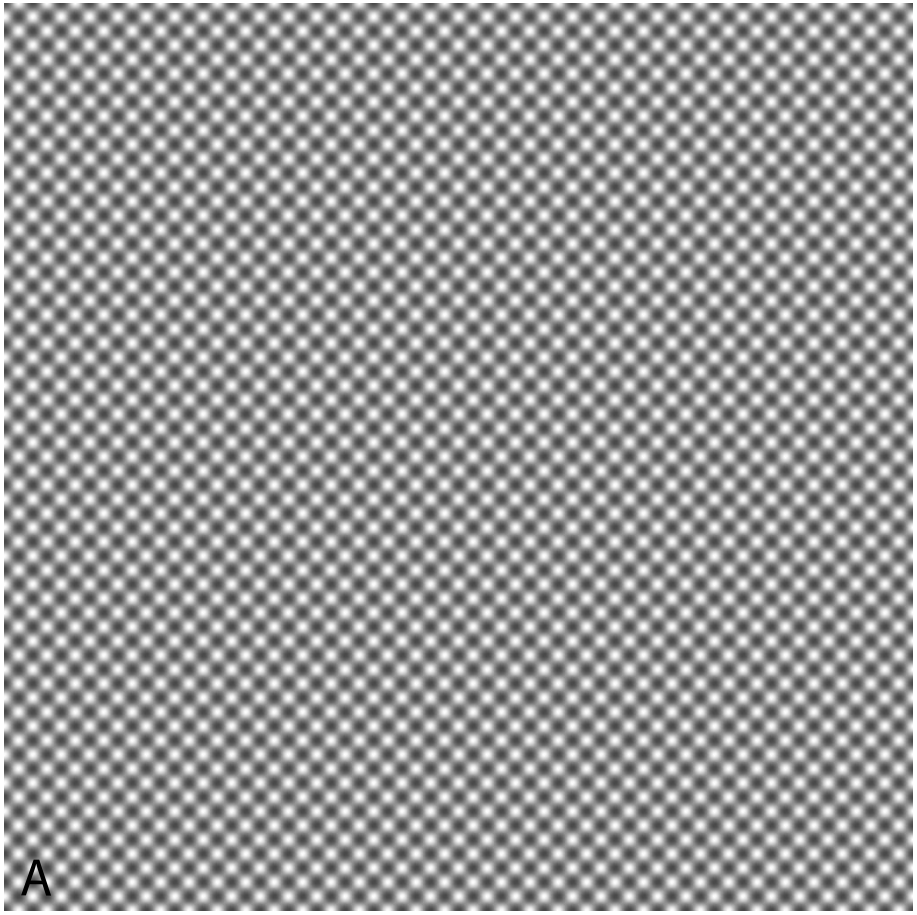

Figure : A: Si [001] simulation.

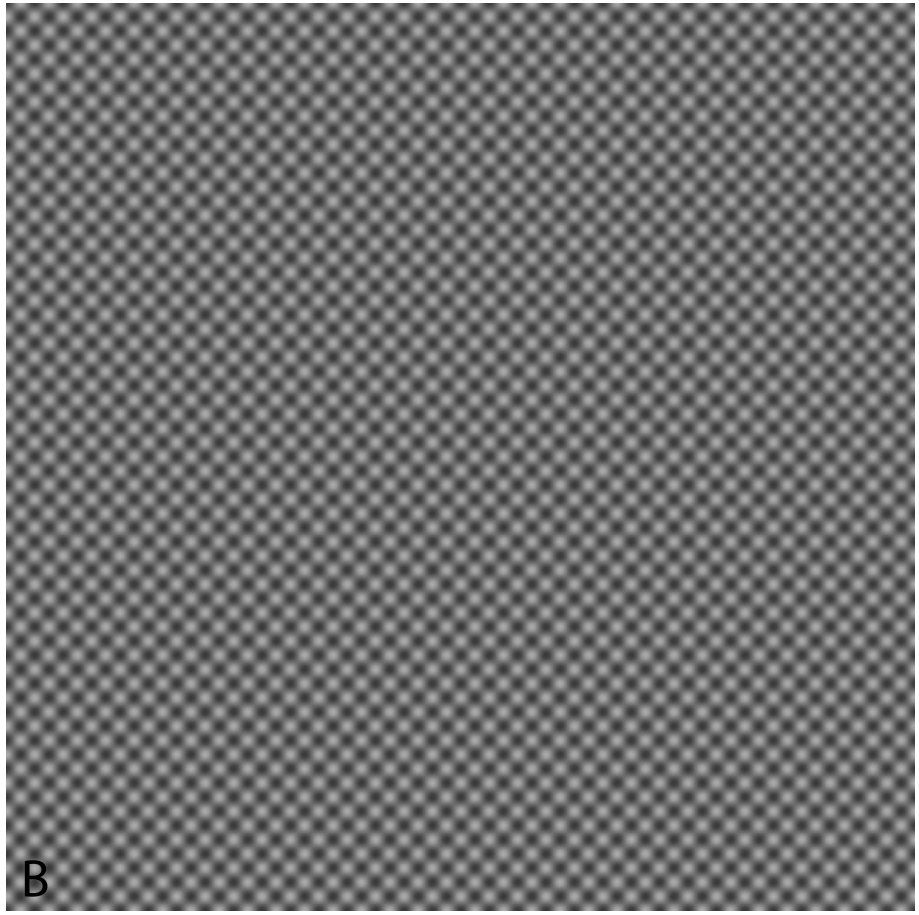

Figure : B: Si [001], simulation + CCD MTF.

CCD MTF: low magnification (225 kx)

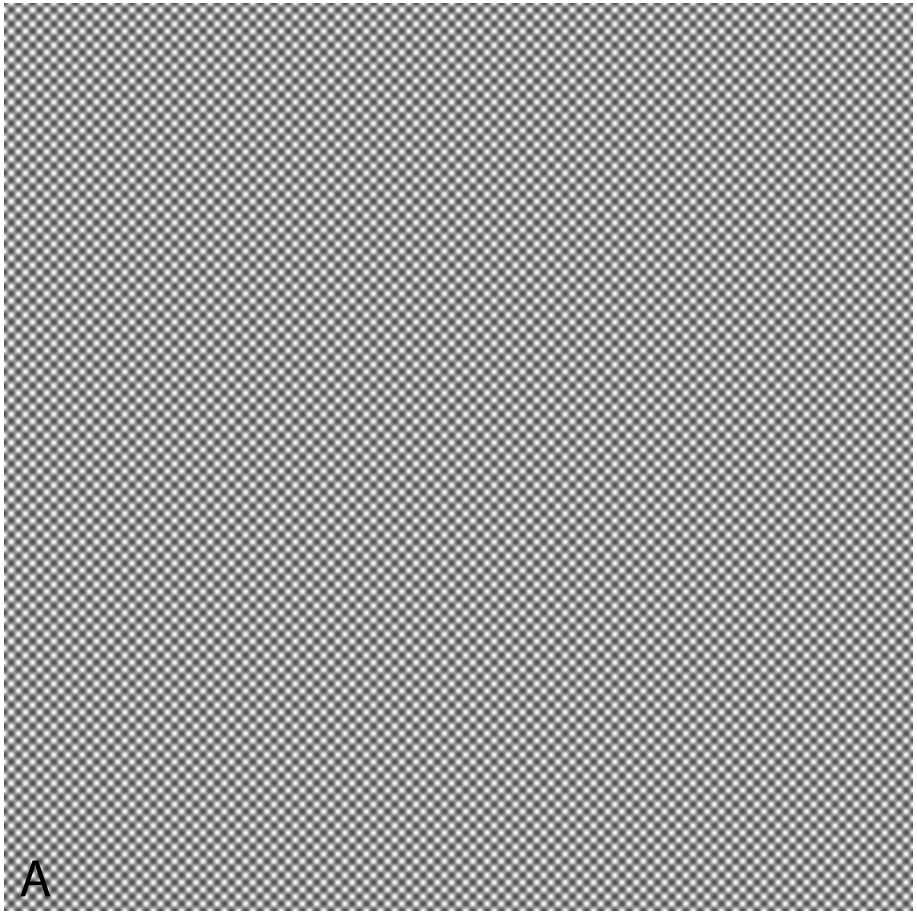

Figure : A: Si [001] simulation.

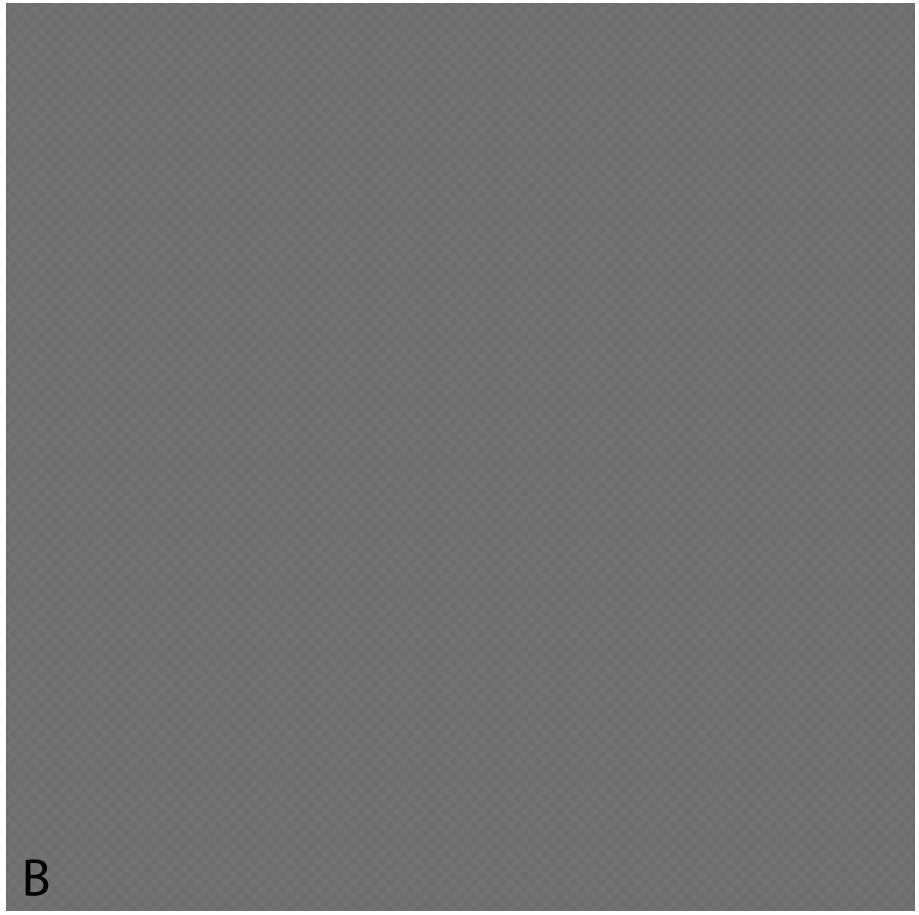

Figure : B: Si [001], simulation + CCD MTF.

HRTEM / HRSTEM problem: electron channeling (ZnTe [110])

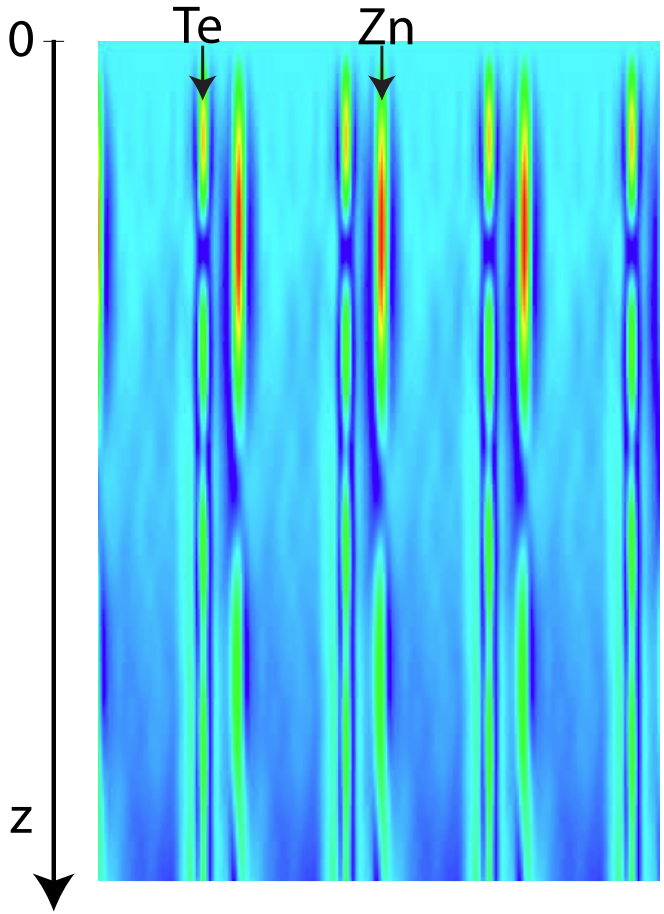

Figure : ZnTe [110] wave function intensity.

Channeling explains several features of HRTEM and STEM images (i.e. appearance / disappearance of contrast of impurities).

Does C_s and C_c correction solves all imaging problems?

Example: CdCu_2, visibility of the 3 Cu atomic columns.

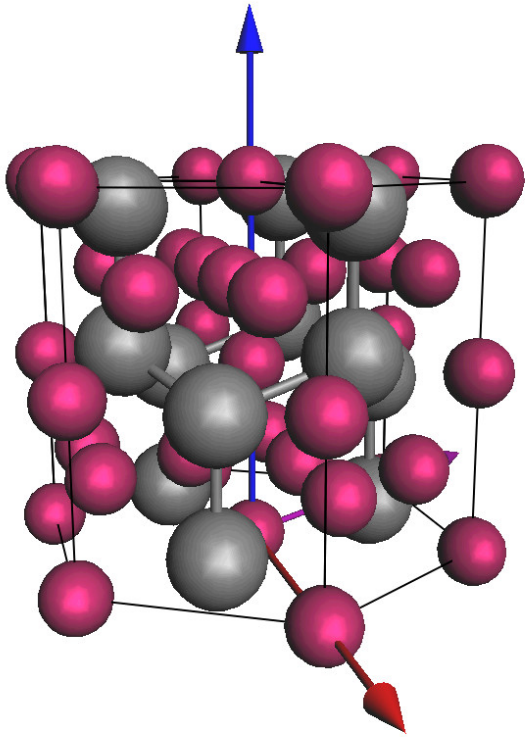

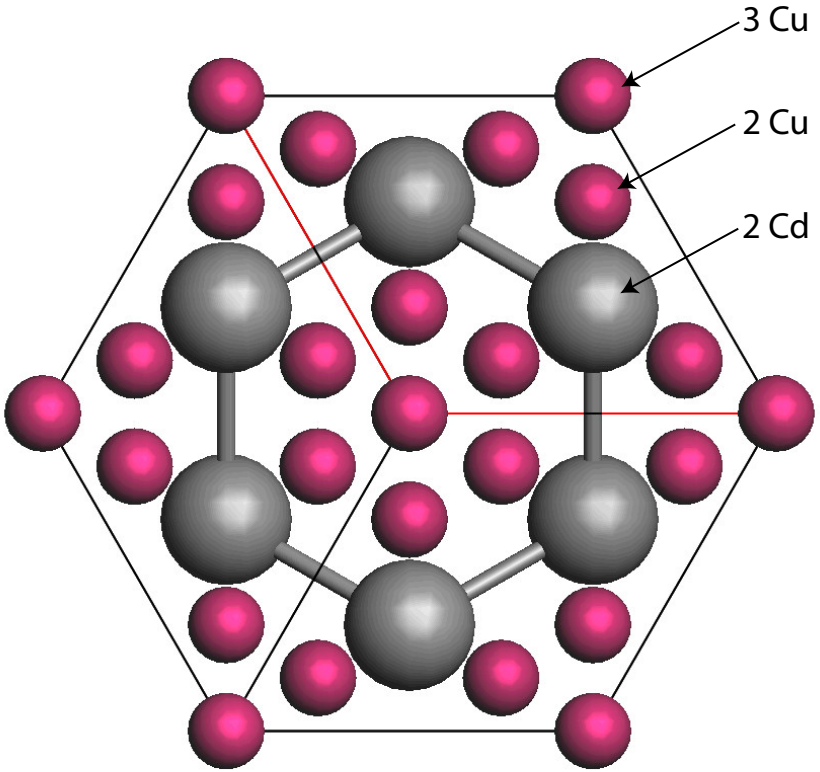

HRTEM image simulation conditions

Acc. [kV]	$C_s[mm]$	$C_5[mm]$	$C_c[mm]$	$\Delta E[eV]$	Z [nm]	$\Delta z[nm]$
300	-0.008	30	0.5	0.6	-4.9	1
300	-0.008	30	0.1	0.2	-2.0	1

Dynamical scattering effects are not affected by C_s and/or C_c corrected TEM!

$CdCu_2[001]$: imaging parameters set 1

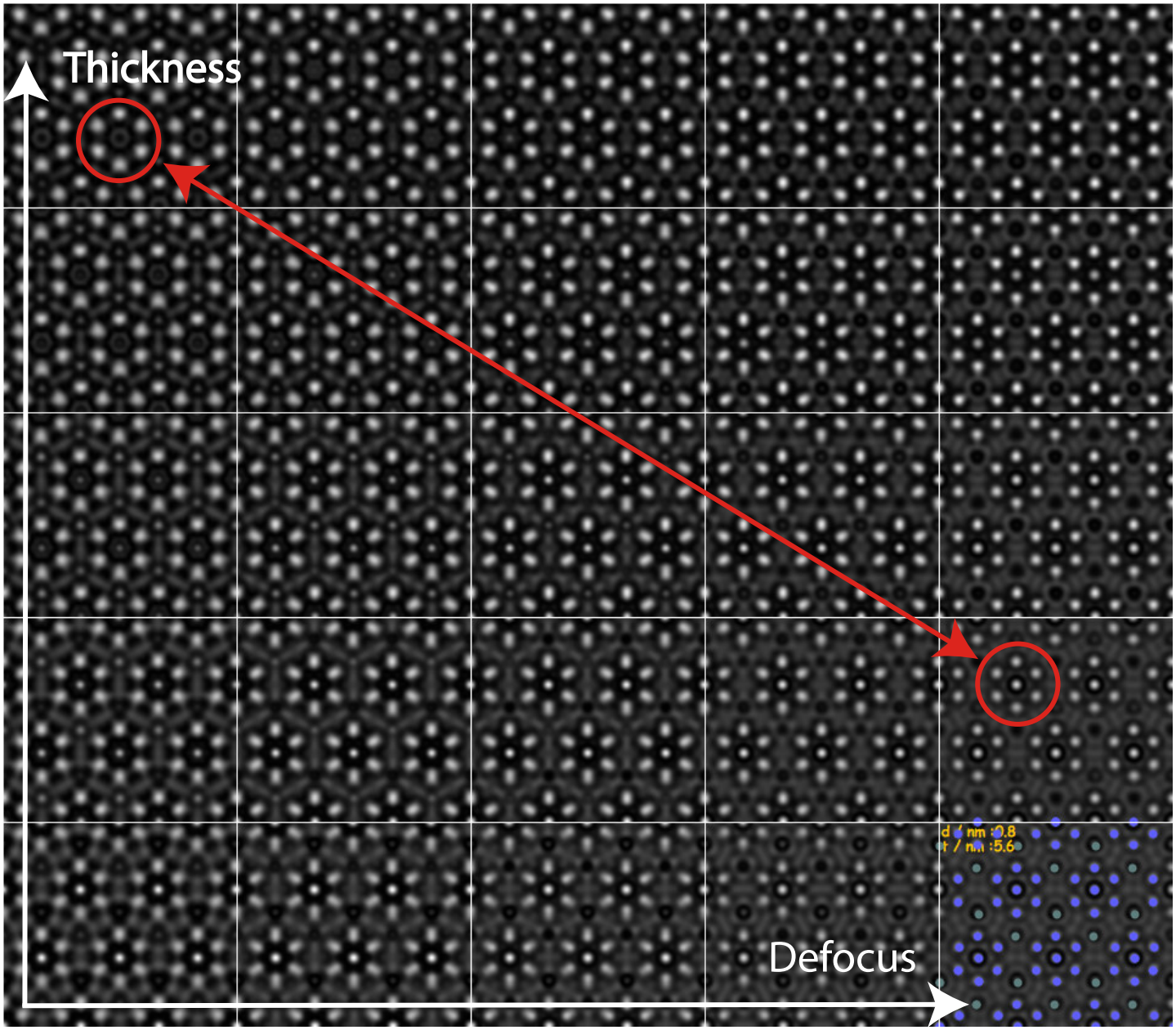

Visibility of 3 Cu atomic columns depends on specimen thickness and defocus.

$CdCu_2[001]$: imaging parameters set 2

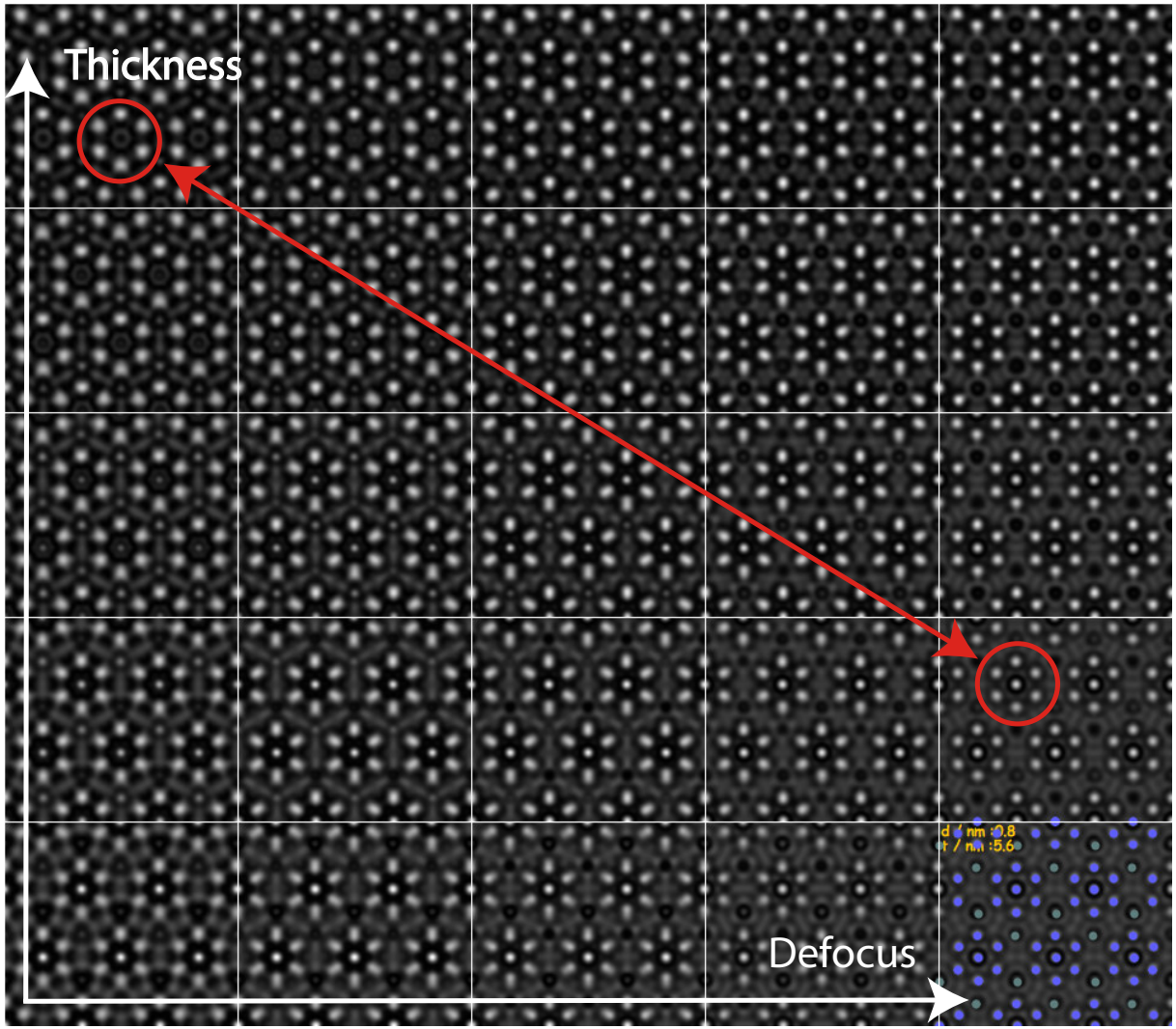

Improving C_c and ΔE does not affect the visibility of 3 the Cu atomic columns. It depends on specimen thickness (and defocus indeed). Visibility of the 3 Cu atomic columns is always affected by dynamical scattering. Only extremely thin specimen ($\leq$ 10 nm) will allow faithful imaging of crystal projected potential.

HRTEM or STEM HAADF imaging

High Angle Annular Dark Field (HAADF): inelastically scattered electrons.
When simulation is necessary how to simulate images?
Numerous approximations:

- Simple projected + convolution with probe intensity: no channeling effect (Weak Object Approximation).
- Multislice calculation: channeling + inelastic scattering (absorption potential) + convolution with probe intensity.
- Frozen lattice (phonon) approximation: atoms of super-cell displaced out of equilibrium position, probe scanned on imaged area, intensity collected by annular detector.
- Pennycook, Nellist, Ishizuka, Shiojiri, Allen, Wang, Rosenauer, van Dyck, ...

Except the first 2 methods, simulation time expensive (luxury?). Approximations (necessity) may suffice...

HAADF: graphene

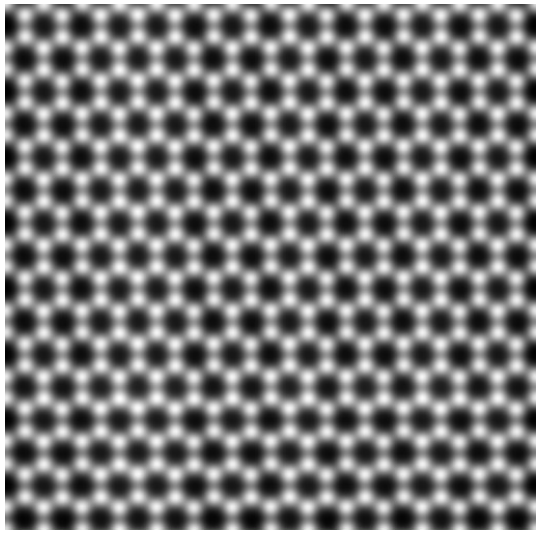

Figure : Proj. pot. approx.

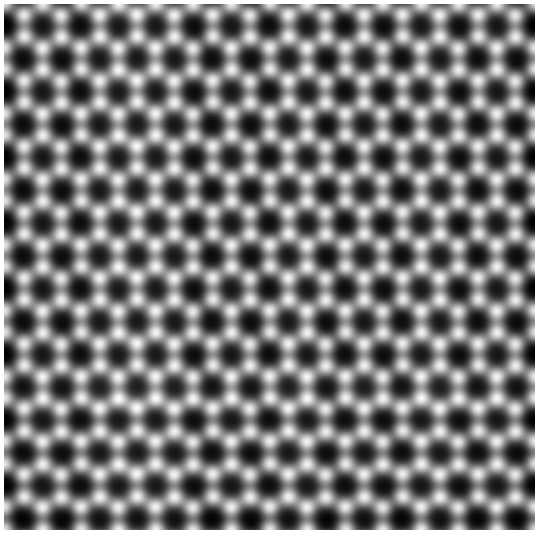

Figure : Channeling calculation.

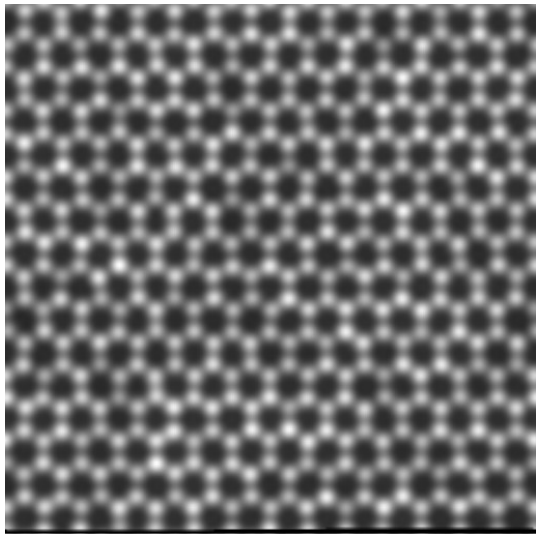

Figure : Frozen lattice 5 conf.

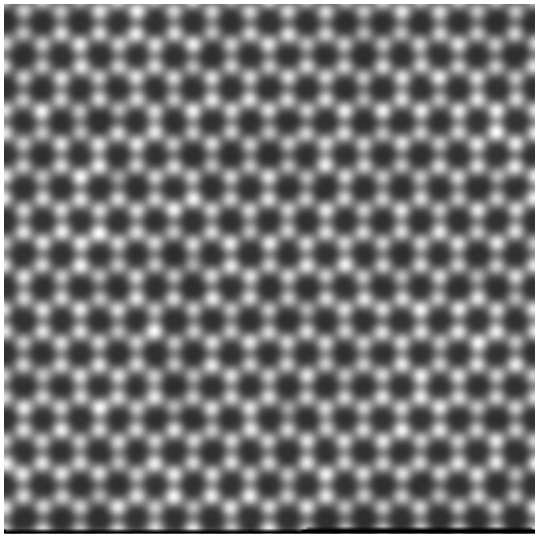

Figure : Frozen lattice 10 conf.

HRSTEM - HRTEM comparison: graphene with add atoms

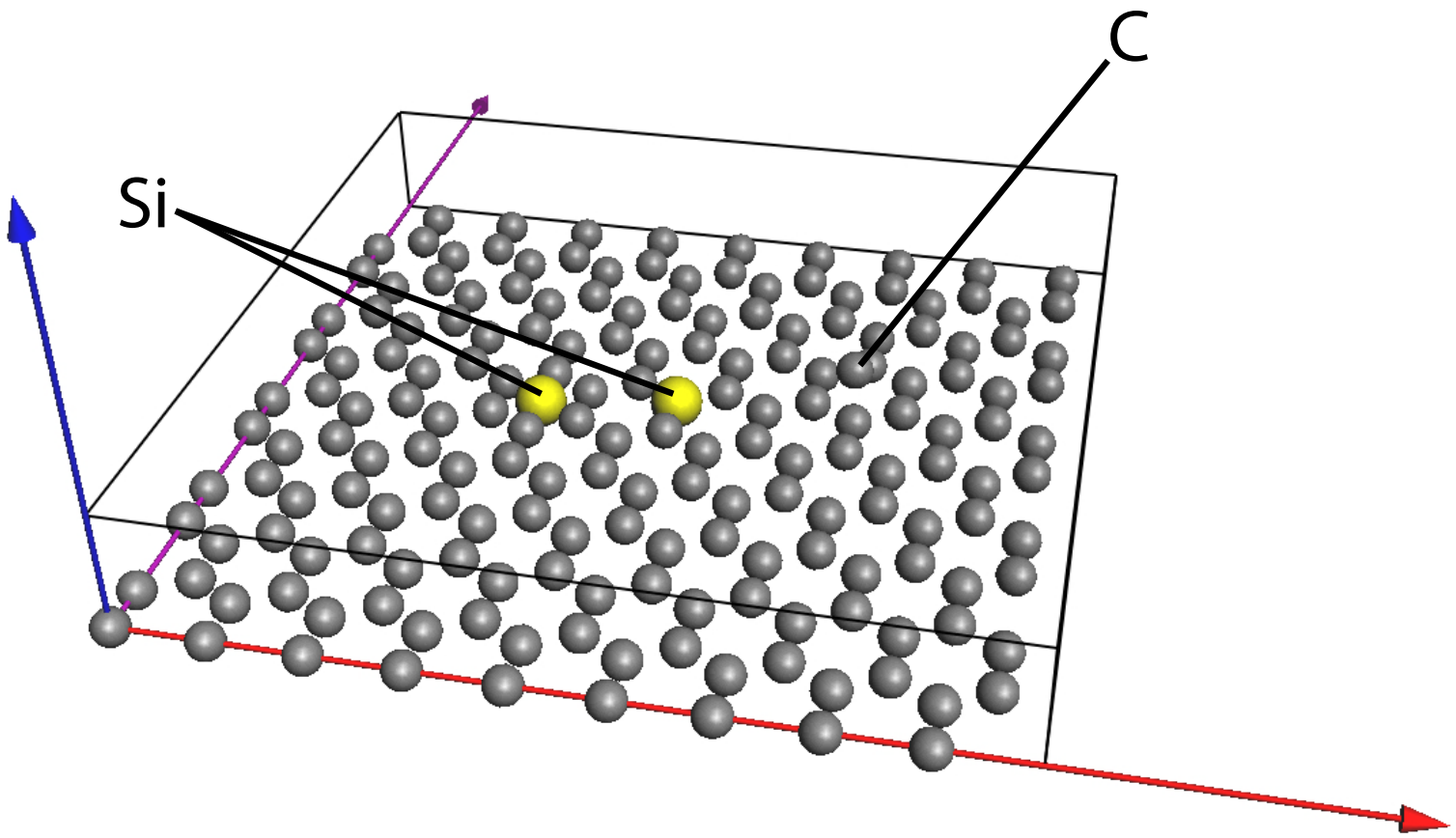

Figure : Graphene with Si in 6 C ring, Si substitutional and 2 C column.

Graphene HAADF (100 kV, 70 -150 mrad)

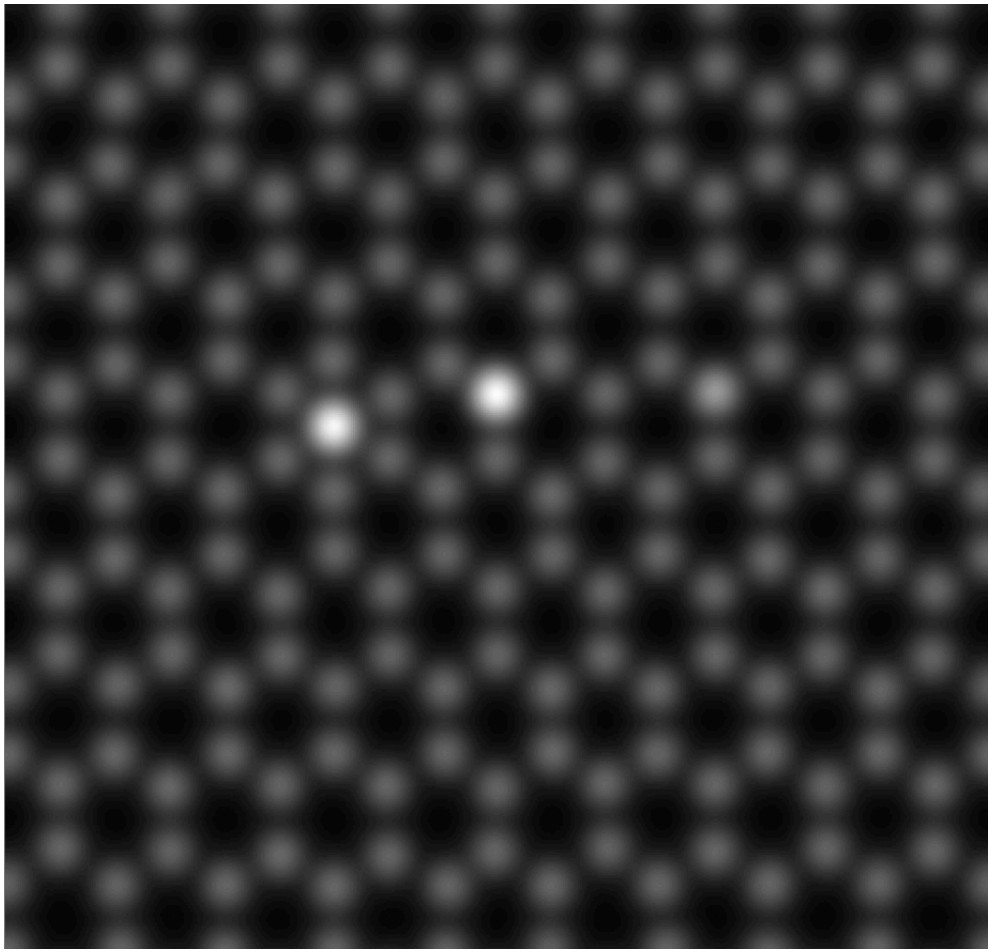

Figure : Frozen lattice (∼400 s).

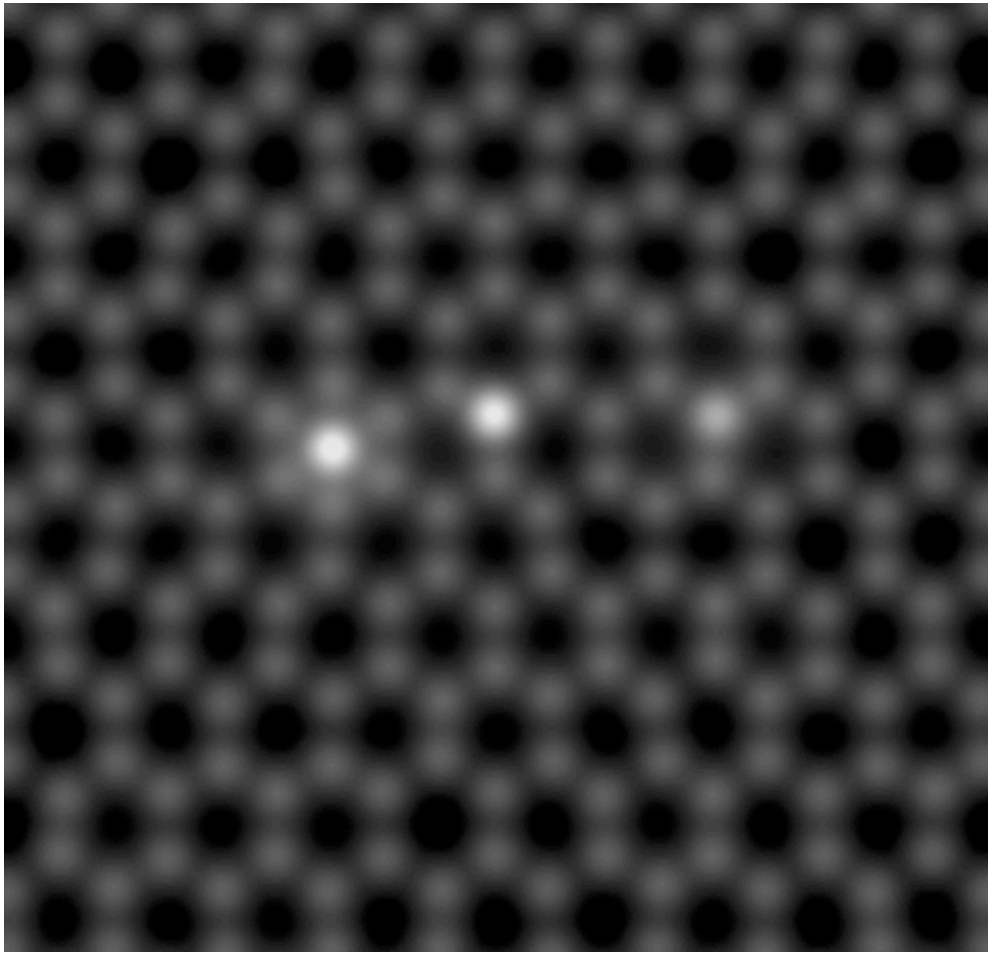

Figure : Channeling (∼2 s).

One Si shows more contrast than 2 C atoms (i $\sim Z^2$) : 14^2 compared to $\sim 2 \times 6^2$.

Graphene HRTEM (100 kV, $C_s - 0.033mm$)

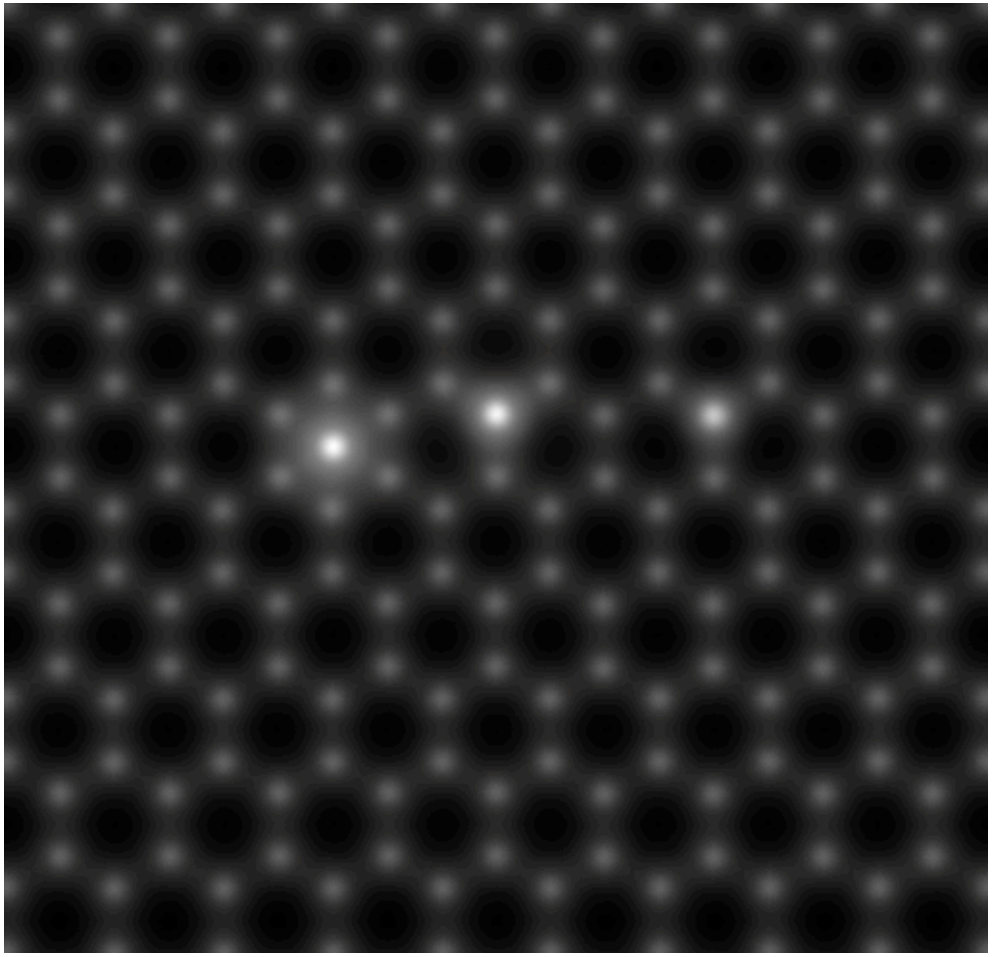

Figure : Weak phase object app., $C_c = 0.5mm$

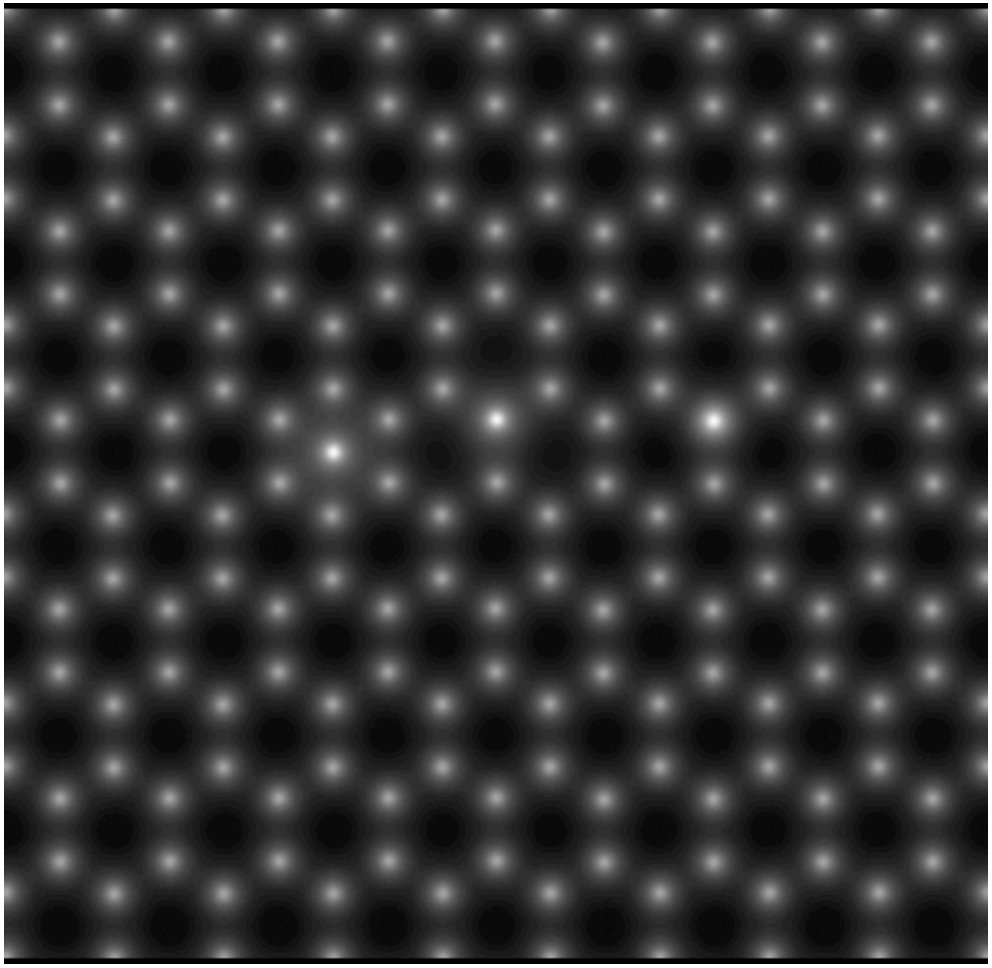

Figure : Multislice, $C_s = -0.033mm$, $C_c = 0$, no thermal magnetic noise.

HRTEM does not display the strong contrast difference between one Si and two C as given by HAADF.

Quantitative HR(S)TEM

Image simulation necessary for quantitative work[15].

- Exit wave function recovery using focal series reconstruction.
- Transport of intensity equation.

But... can also be used for teaching or planing HRTEM/HRSTEM observations.

[15] K. W. Urban, Science **321** (2008) 506.

HRTEM / HRSTEM problem: aberrations of optical system

Reaching 0.05 nm resolution sets very strong conditions on aberrations correction.

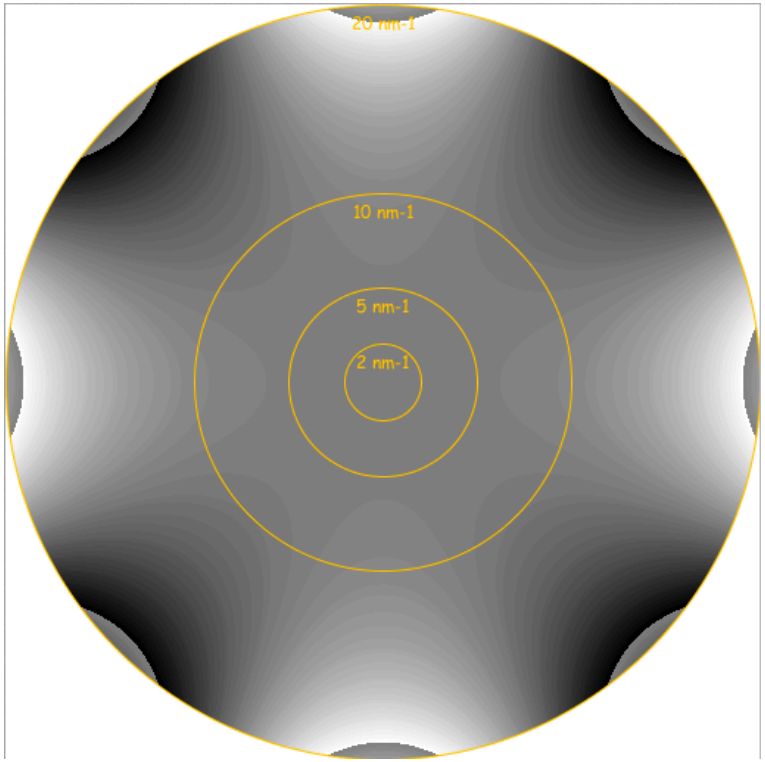

Figure : Aberration figure of $C_{34}(0.5\mu\text{m})$, phase jump at $\frac{\pi}{4}$.

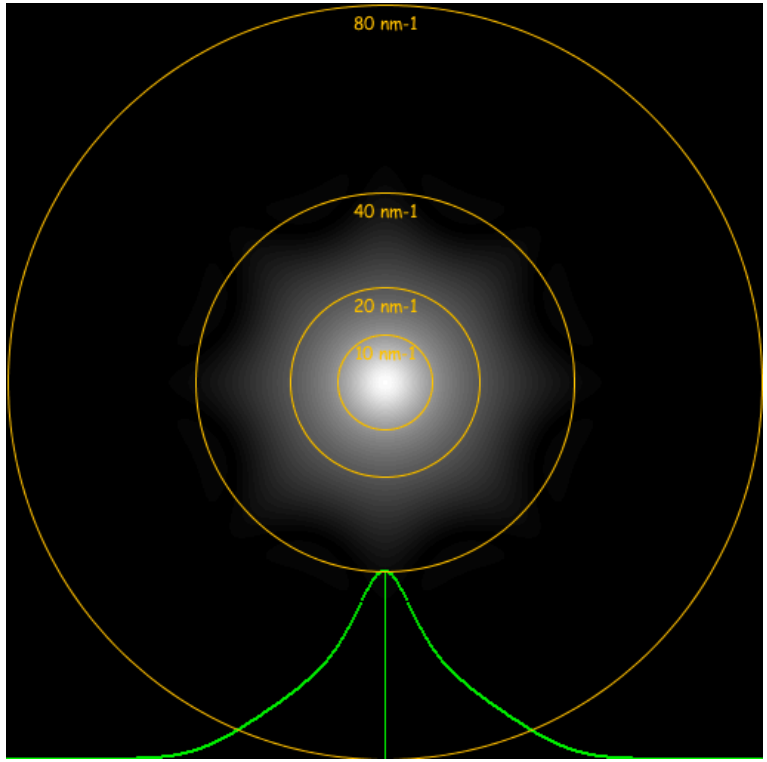

Figure : Optical Transfer Function.

Note that Optical Transfer Function (HRSTEM) transfers higher spatial frequencies than Ccoherent Transfer Function (HRTEM).

HAADF: graphene

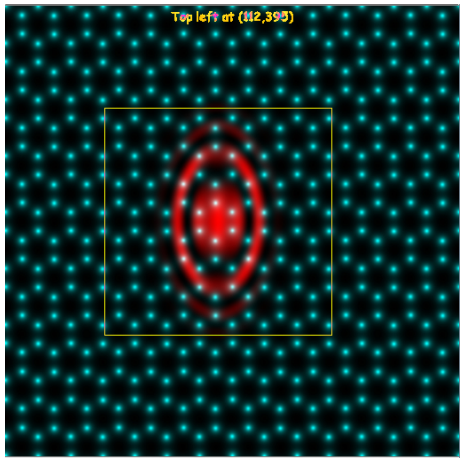

Figure : Probe affected by 2 fold astigmatism.

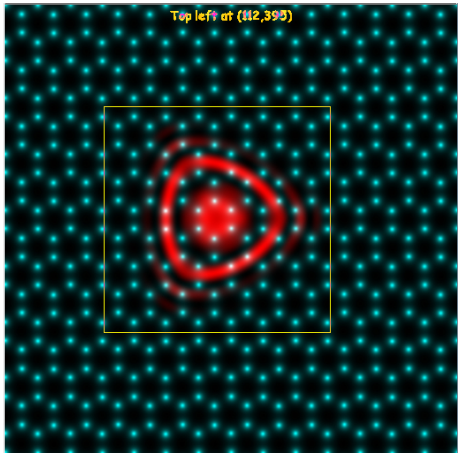

Figure : Probe affected by 3 fold astigmatism.

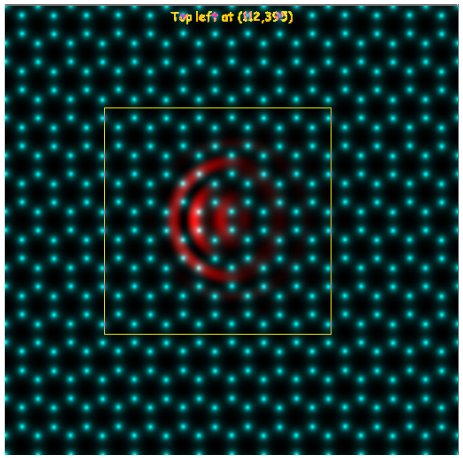

Figure : Probe affected by coma.

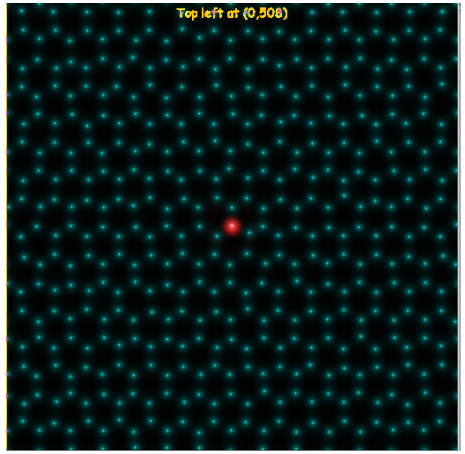

Figure : Corrected probe (best defocus).

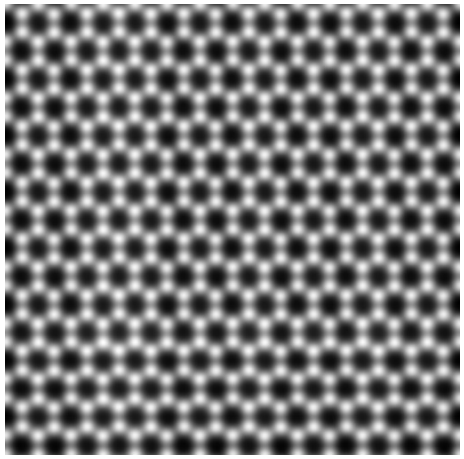

Figure : HAADF projected potential approximation.

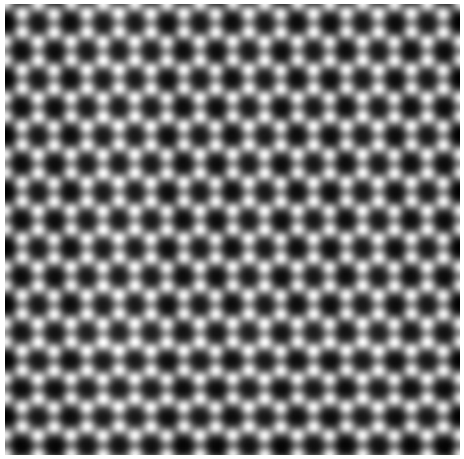

Figure : HAADF multislice calculation (simple).

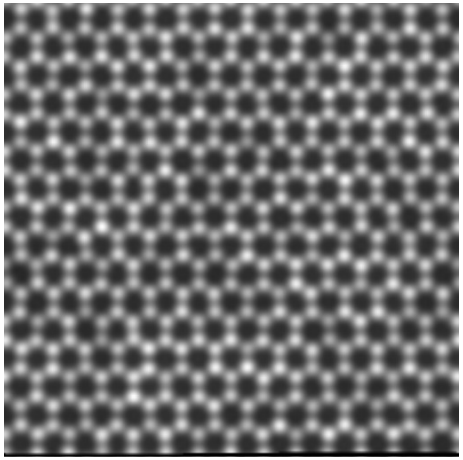

Figure : Frozen phonons 5 configurations.

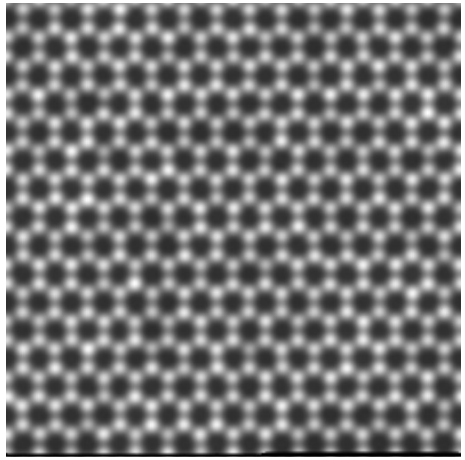

Figure : Frozen phonons 10 configurations.

Appendix 1: Dynamical theory of elastic scattering of high energy electron

We aim to understand in details multiple elastic scattering of electrons by crystals.

- High energy electron (eE).
- Periodic interaction potential $V(\vec{r})$.
- Time independent flux of incident electrons.

The fundamental equation of electron elastic scattering by a potential $V_v\,[Volt]$(positive inside a crystal) in the approximation of a stationary flux of electrons of a given energy $e\,E$ is the Schrödinger equation[16]:

$$\triangle\Phi(\vec{r}) + \frac{2me}{\hbar^2}[E + V_v(\vec{r})]\Phi(\vec{r}) = 0$$

With a change of notation its is written as:

$$[\triangle + 4\pi^2 K_i^2]\ \Phi(\vec{r}) = -4\pi^2 V_v(\vec{r})\ \Phi(\vec{r})$$

Where the wavevector $|\vec{K}_i|$ of the incident electrons is given by:

$$|K_i| = \frac{\sqrt{2meE}}{h}$$

and

$$m = \gamma\ m_0$$

[16] C. Humphreys, The scattering of fast electrons by crystals, Rep. Prog. Phys. **42** (1979) 1825-1887.

Schrödinger equation

The Laplacian $\triangle = \frac{\partial^2}{\partial x^2} + \frac{\partial^2}{\partial y^2} + \frac{\partial^2}{\partial z^2}$ is written as: $\triangle_\rho + \frac{\partial^2}{\partial z^2}$. As a result, $[\triangle + ...]e^{2\pi\imath k_z z}\Psi(\rho; z)$ is given by: $[\triangle_\rho + \frac{\partial^2}{\partial z^2} + ...]e^{2\pi\imath k_z z}\Psi(\rho; z)$.
Performing the z-differentiation:

$$\frac{\partial^2}{\partial z^2}e^{2\pi\imath k_z z}\Psi(\rho; z) = e^{2\pi\imath k_z z}[-4\pi^2 k_z^2 + 4\pi\imath k_z\frac{\partial}{\partial z} + \frac{\partial^2}{\partial z^2}]\Psi(\rho; z)$$

Inserting the last expression and dropping the term $e^{2\pi\imath k_z z}$:

$$[\triangle_\rho + 4\pi^2(K_i^2 - k_z^2 + V(\rho; z)) + 4\pi\imath k_z\frac{\partial}{\partial z} + \frac{\partial^2}{\partial z^2}]\Psi(\rho; z) = 0$$

Since $K_i^2 = k_z^2 + \chi^2$:

$$[\triangle_\rho + 4\pi^2\chi^2 + 4\pi^2 V(\rho; z) + 4\pi\imath k_z\frac{\partial}{\partial z} + \frac{\partial^2}{\partial z^2}]\Psi(\rho; z) = 0$$

Rearranging the last equation:

$$\imath\frac{\partial\Psi(\rho; z)}{\partial z} = -\frac{1}{4\pi k_z}[\triangle_\rho + 4\pi^2\chi^2 + 4\pi^2 V(\rho; z) + \frac{\partial^2}{\partial z^2}]\Psi(\rho; z)$$

Fundamental equation

$$\imath\frac{\partial\Psi(\rho;z)}{\partial z} = -\frac{1}{4\pi k_z}[\triangle_\rho + 4\pi^2\chi^2 + 4\pi^2 V(\rho;z) + \frac{\partial^2}{\partial z^2}]\Psi(\rho;z)$$

The term $|\frac{\partial^2\Psi(\rho;z)}{\partial z^2}|$ being much smaller than $|k_z\frac{\partial\Psi(\rho;z)}{\partial z}|$ we drop it (this is equivalent to neglect backscattering).
Fundamental equation of elastic scattering of high energy mono-kinetic electrons with a potential within the approximation of small angle scattering:

$$\imath\frac{\partial}{\partial z}\Psi(\rho;z) = -\frac{1}{4\pi k_z}[\triangle_\rho + 4\pi^2\chi^2 + 4\pi^2 V(\rho;z)]\Psi(\rho;z)$$

Time dependent Schrödinger equation $\Longrightarrow$ solution by many methods of quantum mechanics!

Remarks

- The approximations of the fundamental equation are equivalent to assume that the scattering potential is small compared to the accelerating potential and that k_z varies only slightly with z. It is in fact a quite good approximation, since the mean crystal potential is of the order of $10 - 20\ V$.
- Electron backscattering is neglected, the electron are moving forwards.
- The fundamental equation is actually equivalent to a 2-dimensional Schrödinger equation ($\rho = \{x, y\}$) where z plays the role of time. The system evolution is causal, from the past to the future.

Fundamental equation in Hamiltonian form:

$$\imath \frac{\partial}{\partial z} \Psi = H\ \psi$$

where:

$$H = -\frac{1}{4\pi k_z}[\triangle_\rho + 4\pi^2\chi^2 + 4\pi^2 V(\rho; z)] = H_o + \frac{4\pi^2 V(\rho; z)}{4\pi k_z}$$

A fundamental postulate of quantum mechanics[17] says that the evolution operator obeys the equation:

$$\imath \frac{\partial}{\partial z} U(z, 0) = H(\rho; z)\ U(z, 0)$$

[17] R. Shankar, Principles of Quantum Mechanics (1994) Plenum Press, New York and London.

Causal evolution operator

$U(z,0)$: unitary operator (the norm of $|\Psi>$ is conserved), in general not directly integrable $\Longrightarrow$ approximations.

$U(z,0)$ can be directly integrated only when $H(\rho;z)$ and $\frac{\partial}{\partial z}H(\rho;z)$ commute. In that case the general solution is[18]:

$$U(z,0) = e^{-\imath \int_0^z H(\tau)\, d\tau}$$

$H(\rho;z)$ and $\frac{\partial}{\partial z}H(\rho;z)$ commute when:

- $V(\rho;z)$ does not depend on z, i.e. $V(\rho;z) = V(\rho)$(perfect crystal).
- $V(\rho;z)$ can be neglected (free space propagation).
- $H(\rho;z)$ is approximated by it potential term (phase object).

Three approximations are available in jems:

- Multislice method.
- Bloch wave method.
- Howie-Whelan column approximation.

[18] A.Messiah, Mecanique quantique (1964) Dunod Paris.